AD-A160 611 THERMAL AND MECHANICAL PROPERTIES OF CALCIUM LANTHANUM SULFIDE(U) SOUTHERN RESEARCH INST BIRMINGHAM AL J R KOENIG APR 85 SORI-EAS-85-401-5267-I-F 1/1

UNCLASSIFIED N00014-83-K-0195 F/G 20/6 NL

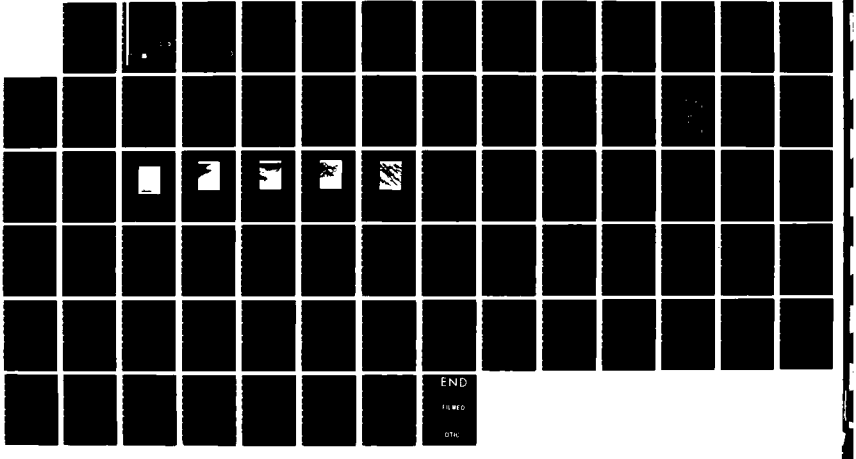

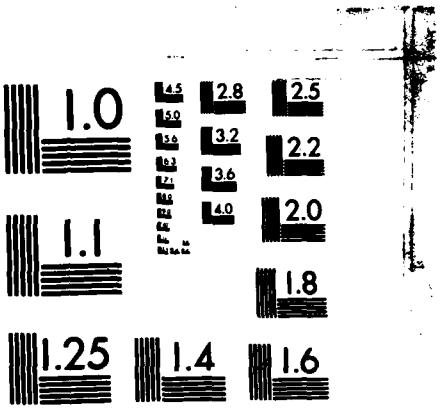

MICROCOPY RESOLUTION TEST CHART
NATIONAL BUREAU OF STANDARDS-1963-A

AD-A160 611

DTIC FILE COPY

SoRI-EAS-85-401-5267-I-F

THERMAL AND MECHANICAL PROPERTIES OF CALCIUM LANTHANUM SULFIDE

Final Report to

OFFICE OF NAVAL RESEARCH
Department of the Navy
800 North Quincy Street
Arlington, Virginia 22217

Contract Number N00014-83-K-0195

April, 1985

DTIC
ELECTE
S OCT 28 1985 D
B

DISTRIBUTION STATEMENT A
Approved for public release;
Distribution Unlimited

Southern Research Institute

85 10 28 006

SoRI-EAS-85-401-5267-I-F

THERMAL AND MECHANICAL PROPERTIES OF CALCIUM LANTHANUM SULFIDE

Final Report to

OFFICE OF NAVAL RESEARCH
Department of the Navy
800 North Quincy Street
Arlington, Virginia 22217

Contract Number N00014-83-K-0195

PREPARED BY:

John R. Koenig

J. R. Koenig, Head
Thermophysical Division

April, 1985
Date

APPROVED BY:

C. D. Pears

C. D. Pears, Director
Mechanical and Material Engineering
Department

Southern Research Institute
2000 Ninth Avenue, South
Post Office Box 55305
Birmingham, Alabama 35255-5305

DTIC
ELECTE
OCT 2 8 1985
S D
B

DISTRIBUTION STATEMENT A
Approved for public release
Distribution Unlimited

TABLE OF CONTENTS

		Page
1.0	INTRODUCTION	1
2.0	APPARATUSES AND PROCEDURES	3
	2.1 Flexure	3
	2.2 Thermal Conductivity	5
	2.3 Thermal Expansion	7
	2.4 Heat Capacity	8
	2.5 Bulk Density	10
	2.6 Ultrasonic Velocity	10
3.0	DATA AND DISCUSSION	11
	3.1 NonDestructive Characterization	11
	3.2 Flexure	11
	3.3 Thermal Expansion	13
	3.4 Specific Heat	13
	3.5 Thermal Conductivity	13
4.0	SUMMARY OF THE DATA	14
5.0	REFERENCES	15
Appendices		
	A - Flexural Load/Deflection Curves	A- 1
	B - Sensitivity Studies	B-23

LIST OF ILLUSTRATIONS

Figure		Page
1	Schematic of High Temperature Flexural Apparatus	16
2	Flexural Four-Point Loading Set-up	17
3	Schematic of Comparative Rod Thermal Conductivity Apparatus	18
4	Assembly of Quartz Tube Dilatometer for Thermal Expansion Measurements	19
5	Block Diagram of Ultrasonic Velocity Measuring Apparatus	20
6	Flexural Specimen Configuration	21
7	Flexural Moduli of $CaLa_2S_4$ as a Function of Temperature	22
8	Strength versus Temperature for $CaLa_2S_4$	23
9	EDS Scan of $CaLa_2S_4$ Specimen Fracture Face	24
10	Failure Surface of F-10	25
11	Probable Initiation Site in F-10	26
12	Higher Magnification of Probable Initiation Site in F-10	27
13	Structure in "Hackle" seen in Figure 10	28
14	Thermal Specimen Configurations	29
15	Thermal Expansion of $CaLa_2S_4$	30
16	Enthalpy Plot for $CaLa_2S_4$	31
17	Specific Heat of $CaLa_2S_4$	32
18	Thermal Conductivity of $CaLa_2S_4$	33

Accession For
NTIS GRA&I
DTIC TAB
Unannounced
Justification
By PER LETTER
Distribution/
Availability Codes
Dist | Avail and/or Special
A-1

QUALITY INSPECTED 4

LIST OF TABLES

Table		Page
1	Test Matrix for $CaLa_2S_4$	34
2	Density and Velocity of $CaLa_2S_4$ Specimens	35
3	Flexural Properties of $CaLa_2S_4$ IR Window Material	36
4	Thermal Expansion of $CaLa_2S_4$ - Encl 4 Measured in Quartz Dilatometer	37
5	Thermal Expansion of $CaLa_2S_4$ - Encl 4 Measured in Quartz Dilatometer	38
6	Enthalpy of $CaLa_2S_4$ Measured in the Adiabatic Calorimeter	39
7	Enthalpy of $CaLa_2S_4$ Measured in the Ice Calorimeter	40
8	Thermal Conductivity of $CaLa_2S_4$ - Encl 6 using Comparative Rod Apparatus with TM-Silica References	41
9	Thermal Conductivity of $CaLa_2S_4$ - Encl 6 using Comparative Rod Apparatus with TM-Silica References	42
10	Thermal Conductivity of $CaLa_2S_4$ - Encl 6 using Comparative Rod Apparatus with TM-Silica References	43
11	Thermal Conductivity of $CaLa_2S_4$ - Encl 6 using Comparative Rod Apparatus with TM-Silica References	44
12	Summary of $CaLa_2S_4$ Mechanical and Thermal Data	45

THERMAL AND MECHANICAL PROPERTIES OF CALCIUM LANTHANIUM SULFIDE

1.0 INTRODUCTION

This is the final report of the effort conducted at Southern Research Institute for the Office of Naval Research, Arlington, Virginia, under contract number N00014-83-K-0195. The purpose of this effort was the determination of the mechanical and thermal properties of specimens fabricated from calcium lanthanium sulfide ($CaLa_2S_4$) by Raytheon Company, Research Division.

The $CaLa_2S_4$ was reported by Raytheon to have initial (slow) decomposition occurring at 700 to 800 °C. They suggested 1000 °C as an effective use temperature. It melts at 1800 °C. It is further reported to have favorable transmission properties in the 8-12 micron range and twice the hardness of ZnS.[1]

The test matrix used is shown in Table 1. It is essentially identical to the test matrix utilized for the evaluation of ZnS and ZnSe under NWC contract number N60530-83-C-0031 and reported in SoRI-EAS-84-1096, Thermal and Mechanical Properties of Candidate Optical Materials for IR windows. It was designed to obtain sufficient information for comparative design studies and screening of the material with emphasis on those properties which are anticipated to be most critical for a thermostructural environment.

The thermal stress resistance was investigated using thermal expansion, thermal conductivity, specific heat and flexure. Sensitivity

studies conducted on this class of materials (reference 2, see Appendix B) show the critical properties which control the thermal stress reponse for the general heating rates and geometries of interest here to be the thermal expansion, tensile strength or strain to failure and the ratio of the high temperature compressive modulus to low temperature tensile modulus. The other properties measured have a second order effect on the thermal stress response, but are important for other critical responses. For example, the thermal conductivity and specific heat, in addition to being necessary to predict the thermal fields for thermal stress prediction, also affect in depth heating of other system components and with the thermal expansion, aid in thermal deformation compatibility design with the collar. In addition to these properties, nondestructive measurements (NDC) were made to aid the interpretation of the data and fractographic studies were made of the tested specimens to aid in the understanding of the results.

Tensile and compressive tests, which were planned in the initial matrix, were not conducted as specimens were not received. This is unfortunate, particularly for the tensile tests, as these are more directly related to the response of the material as a dome under thermostructural loading than are the flexural results.

The flexure tests were conducted at a series of temperatures providing both flexural modulus and strength. Tests were conducted at 70, 500, 1000, 1500 and 1800 °F. (20, 260, 538, 816 and 982 °C). Thermal expansion and specific heat were measured up to the material limit (~1000 °C). Thermal conductivity was measured up to about 650 °C at which temperature the degradation of the material poisoned the thermocouples and additional data could not be taken. Several attempts to extend that range meet with limited success as will be discussed later.

The nondestructive tests consisted of measuring the bulk density and sonic velocity of each specimen plus a careful visual examination. The surface roughness was inspected using optical and SEM microscopy. SEM microscopy was used for the fractography.

2.0 APPARATUSES AND PROCEDURES

2.1 Flexure

Beam flexural evaluations were performed in the flexural apparatus shown in Figure 1 which consists of a load frame, load cell, load train, graphite resistance furnace, deflection measurement system and associated equipment for continuous measurement of load and deflection. Load was applied to the specimen from the lower end of the load train, and load measurements are made by the load cell at the upper end. As the load is applied to the specimen midpoint, deflection of the specimen is measured by means of a rod contacting the specimen midpoint and extending down to a differential transformer. The differential transformer is supported by a tube that attaches to the support bar eliminating load train motion from the deflection measurement. A new molybdinum loading system was designed and fabricated for this effort.

From the plot of load versus midpoint deflection, the values of modulus of rupture and flexural measured. The ultimate strength is calculated from the equation:

$$S = \frac{Mc}{I}$$

which simplifies to

$$S = \frac{PL}{bh}$$

for a specimen with a rectangular cross-section employing the third span loading method, and where fracture occurs within the middle one third of the specimen span length. The four point loading system is shown schematically in Figure 2. In these equations:

S = modulus of rupture

P = maximum applied load

L = span length

b = width of specimen

h = height of the specimen

The initial modulus in flexure was calculated from the equation:

$$E_f = \frac{6P\ [a^3\ 3 + ac/2\ (a + c/4]}{\delta\ bh^3}$$

where

E_f = elastic modulus in flexure

P/δ = ratio of load to corrected midpoint deflection at any point along the elastic portion of the curve

a and c = distances between the supports and loading points

The above equation neglects the deformation due to shear and assumes that the neutral axis coincides with the center of the cross-section.

2.2 Thermal Conductivity

The apparatus used for the evaluation of the thermal conductivity of these materials through 1800 °F was the comparative rod apparatus (CRA). The CRA compares the conductivity of the specimen being characterized to the known conductivity of a reference piece. Several types of references are available and their conductivities are traceable to NBS data or other reliable sources. In this effort references of Pyroceram and slipcast fused silica were used.

The CRA consists of a series of cylindrical pieces stacked in a vertical column as illustrated in Figure 3. The specimen and reference pieces are placed in the order reference-specimen-reference. Above the top reference is an electric heater that serves as the heat source for the thermal gradient in the experiment. AlSiMag insulators are placed above the heater and a steel rod forms the top of the column, receiving a compaction weight through a steel ball. Below the bottom reference is another electric heater or insulator, another steel rod, and a cooling sink, if required. The entire column is supported upon a steel ball for elimination of lateral forces that could deform the structure.

In assembling the apparatus, a large annular shell of alumina or transite is moved down around the stacked pieces. The central core of the shell is wound with five electric coils which are guard heaters, each separately controlled to match the temperature gradient through the stacked column, thereby controlling radial heat losses or shunting.

The annular space between the central core and the stacked column is filled with diatomaceous earth, thermatomic carbon, or other insulating material selected to be compatible with the specimen. The entire shell is also filled with insulation. In this case the insulation was thermatomic carbon.

Thermocouples are used to measure temperatures at all key points in the apparatus, including typically three points in the references and specimens, two points in the upper and lower guards, and one point in the middle guard.

For specimens with a conductivity of greater than 10 Btu-in./hr-ft-°F, the temperature gradient through the column is considered to be linear and the radial heat losses to be negligible. The calculations are made in a straightforward manner from Fourier's equation for one dimensional heat flow:

$$q'' = \Delta t \, k/l$$

where q'' = heat flow through the material

Δt = temperature drop across the gage section

k = conductivity of the piece

l = gage length of the piece

The heat flow is calculated for the reference pieces directly since their conductivities are known and the temperature drops and gage

lengths have been measured. It is then solved for the conductivity of the specimen using the arithmetic average of the q" of the upper and lower references.

2.3 Thermal Expansion

Thermal expansion measurements were made using quartz tube dilatometers modified from the Bureau of Standards design for measurements up to 1800 °F. Improvements have been made to prevent lateral movement of the quartz tube, thus eliminating possible erroneous readings.

The specimen was placed in a quartz tube that is firmly secured to the body of the apparatus,which is mounted on a work bench. A second quartz tube of slightly smaller diameter was inserted into the outer tube such that it rests on the specimen end. A quartz rod that is free to move vertically was then placed into the apparatus such that one end is in contact with the dial gage piston. The body of the dial gage was firmly attached to the apparatus. Any expansion or contraction of the specimen is transferred through the inner quartz tube, the quartz push rod, and the dial gage piston to register a displacement on the gage. The quartz tube and specimen are located within a cylindrical electrical heater and can be heated to 1800 °F in the apparatus. The dial gage is calibrated in 0.0001 inch displacements and has an accuracy of ±0.0001 inch at any point in its range (0.5 inches).

The use of quartz for both the fixed and movable parts of the apparatus eliminates any difference in expansion rates and allows the apparatus to record only the expansion or contraction of the specimen. The recorded raw data are then corrected based on calibration data for that dilatometer developed from regular calibration runs on traceable standards.

This facility is shown schematically in Figure 4.

2.4 Heat Capacity

The heat capacity to 1000 °F was determined from data obtained in an adiabatic calorimeter. In this apparatus the heated specimen was dropped into a thermally guarded, calibrated cup, and the enthalpy is measured as a function of the increase in temperature of the cup. The heat capacity is the slope of the enthalpy-temperature curve.

A tubular furnace was used to bring the specimen to temperature. The furnace pivots over the cup allowing the unit also to be used with a cold box for temperatures down to -300 °F. When the furnace is in place and the desired temperature is reached, the specimen is released from a suspension assembly which is triggered externally. Thermocouples are used to measure the specimen temperature.

Specimens of the material were heated to the desired temperature, and following a stabilization period, are dropped into the calorimeter cup. Adiabatic conditions are maintained during each run by manually adjusting the cup guard bath temperature.

The covered cup of the calorimeter is approximately 2.5 inches diameter by 2 inches deep. Three thermocouple wells are located in the bottom wall of the cup. The cup is mounted on cork supports, which rest in a silver plated copper jacket. The jacket is immersed in a bath of ethylene glycol, which is maintained at the temperature of the cup by means of a heater and copper cooling coils immersed in the liquid. A double bladed stirrer

maintains uniform bath temperature.

In the calorimeter six copper-constantan thermocouples, differentially connected between calorimeter cup and jacket, indicate temperature difference between the cup and bath. The six thermocouples allow a difference of 0.03 °F to be detected. This difference is maintained to within 0.15 °F. During the run, absolute temperature measurements of the cup are determined by means of the three thermocouple junctions, series connected, in the bottom of the calorimeter cup.

The enthalpy of the specimen at any initial temperature is calculated from the equation:

$$h = K/W_S \ (t_2 - t_1)$$

where h = enthalpy above t_2

K = calorimeter constant, 0.2654 Btu/°F

W_S = sample weight in lbs

t_1 = initial cup temperature in °F

t_2 = final cup temperature in °F

The calorimeter constant of 0.2654 Btu/°F was determined by measuring the enthalpy of an electrolytic copper specimen of known specific heat. The enthalpy is referred to a common base temperature of 85 °F using linear interpolation. The enthalpy-temperature curve established is used to

determine heat capacity (specific heat) by measuring its slope at different temperatures. This is done both graphically and by analytical methods.

The accuracy of the apparatus has been confirmed by measuring the enthalpy of sapphire (SRM 734 from NBS) and other data which indicate that the overall uncertainty of the apparatus is ±3 percent.

2.5 Bulk Density

The bulk density of the specimens was measured on the specimens by gravimetric techniques. The specimens were measured with micrometers and weighed on a Mettler balance. The reported density is simply the mass, in grams, divided by the calculated volume in cubic centimeters.

2.6 Ultrasonic Velocity

The ultrasonic velocity was measured on each of the specimens in the direction of test. The measurement was made using a through transmission technique. The setup is shown schematically in Figure 5.

The basic apparatuses used for measuring ultrasonic velocity were a Sperry UM 721 Reflectoscope and a Tektronix oscilloscope. In using the through transmission, elapsed time technique for measuring velocity, a short pulse of longitudinal mode sound was transmitted through the specimen. An electrical pulse from the pulse generator was applied to the crystal in the transducer. The pulse generated by the transducer was transmitted through a short delay line and inserted into the specimen. The time of insertion of the leading edge of this sound beam was the reference point on the time base of the oscilloscope which was used as a high speed stop watch. When the leading

edge of this pulse of energy reaches the second transducer it was displayed on an oscilloscope. The difference between the entrance and exit times was used with the specimen length to calculate the sonic velocity.

3.0 DATA AND DISCUSSION

3.1 NonDestructive Characterization

Table 2 shows the bulk density and ultrasonic velocity of each of the specimens tested under this effort. Note that some of the specimens received earlier (thermal specimens) were of slightly lower density than the bulk of the specimens. The average density was 4.611 gms/cc. The sonic velocity was typically 0.201 in./μsec. From these data a sonic modulus (neglecting Poisson's effect) can be calculated. It was typically 17.5 x 10^6 psi. Visual inspect saw no obvious defects except a few chips previously noted by Raytheon.

3.2 Flexure

The flexural test results are provided in Table 3. The tests were run on specimens as shown in Figure 6 with a 1.25 inch inner span and a 3.75 inch outer span. As requested the tensile face was opposite the marked face. This face was reported to have the better finish.

The 70 °F flexural strength was not very high, averaging 7240 psi. This was less than the value reported by Raytheon of about 14000 psi. A large portion of that difference may be attributable to specimen size, the Raytheon data having been generated on miniature specimens. The average 70°

flexural modulus was 13.57 x 10^6 psi. Note that prior to every test a nondestructive mechanical (low stress loading, 1200 psi) test was run at 70° to get an initial modulus). The average value for all the NDM tests was 13.48 x 10^6 psi, in good agreement with the average of the five 70° tests. The modulus is also in fair agreement with the calculated sonic modulus. The elevated temperature moduli show a steady decrease as a function of temperature. This is shown in Figure 7. At 1500 and 1800 °F the data became somewhat nonlinear and were represented by a bilinear fit. The secondary slope is shown as solid symbols on Figure 7 and an effective yield point provided in Table 3. The ultimate flexural strength as a function of temperature is shown in Figure 8. The strength drops slightly or is almost constant (eliminating the weakest specimen brings the average 500° strength to 6750 psi) through 1000 °F then has higher strengths at 1500 and 1800 °F. The higher strengths at 1500 and 1800 °F are concurrent with the nonlinearity of the flexural response curve.

The failures occurred at relatively low levels giving poorly defined fracture patterns. There were zones in the material which gave the appearance of being a visually more absorptive precipitate. These were present in all specimens but became more distinctive as the specimens had seen temperatures of 1000° and over. Also, specimens of that temperature range emitted a distinctive sulphurous order. EDS scans showed these "precipitate" zones to have the same elemental components as the other zones of the specimens. Only calcium, lanthanum and sulfur were detected as illustrated in Figure 9. Figures 10 through 13 show scanning electron microscopy documentation of the fracture initiation site in FS 10, one of the weaker 70 °F flexure tests. Most but not all of the specimens were even less definitive. There is the appearance of a mirror zone and some hackle in the left tensile corner of the specimen seen in Figure 10. The initiation site

(Figures 11 and 12) does not show any defect structure. It was in a "precipitate" zone. Figure 13 shows the structure in the hackle.

The raw load deflection curves are given in Appendix A.

3.3 Thermal Expansion

Figure 14 shows the specimen used for measuring the thermal expansion of the $CaLa_2S_4$. The measured response is shown in Figure 15 and the data given in Tables 4 and 5. The thermal expansion is higher than 0° sapphire which is shown as a reference. Above 1000° a sulfur odor was noted. There was also a slight deviation between the specimens at that temperature range. The two specimens both returned to near zero residual change after cooldown to room temperature. No significant weight loss was noted.

3.4 Specific Heat

Figure 16 shows the enthalpy plot generated for the $CaLa_2S_4$ specimens. Higher scatter than normal was seen above 1100 °F. Also the specimens tended to shatter due to thermal stresses when dropped from the higher temperatures. The calculated specific heat (slope of the curve in Figure 16) is shown in Figure 17. The material has a remarkably low specific heat typical of lanthanum compounds. It rises gradually through about 1200 °F then somewhat more rapidly thereafter. Tables 6 and 7 show the data obtained.

3.5 Thermal Conductivity

The thermal conductivity data generated on the $CaLa_2S_4$ material are shown in Figure 18. The initial data were well behaved at low

temperatures. However, at about 1000 °F on the first run the measured conductivity climbed dramatically and became erratic. Upon return to about 200 °F the data repeated fairly well for the one, lower temperature, specimen. Thermocouples could not be read on the other specimen and upon inspection it was seen that the thermocouples had been destroyed. New thermocouples were installed and cemented in place to protect them. The runs were repeated with similar results, this time obtaining an apparently valid data point at just in excess of 1000 °F. Again the thermocouples were destroyed. As with the expansion, a sulfurous order was detected. It was still present on the specimens after cooldown. No significant weight change was noted.

A third attempt was made this time changing to Pyroceram references with large (10 mil) thermocouple wire. It was planned to extrapolate surface temperatures as a backup after the failure of the internal thermocouples. The results showed permanent change in the conductivity of the material even at room temperature. Again the thermocouples were destroyed including those in the Pyroceram hot reference. Additional data were obtained by extrapolating temperatures to the surface for calculation of the temperature drop across the specimen. Figure 18 shows the apparently valid data only. A line value through the data up to 1000 °F is provided. Tables 8 through 11 provide the measured data.

4.0 SUMMARY OF THE DATA

Table 12 gives a summary of the data and compares the data with ZnS and ZnSe data from NWC Contract N60530-83-C-0031. The strength was somewhat lower and the modulus slightly higher than the ZnS. The comparison to ZnSe was similar except that at 70 °F the strength of the $CaLa_2S_4$ was

slightly higher. Specific heat was slightly lower than the comparison materials but all had low specific heats, the density was intermediate and, as expected from the moduli and densities, the sonic velocity was similar. The most remarkable differences were in the thermal conductivity and thermal expansion. The thermal conductivity is dramatically lower (a factor of about five) than either of the materials and the thermal expansion was a factor of about two higher.

This combination of properties will give a material that is not very good in thermostructural response, as was indicated by the fracturing of the heat capacity specimens, and therefore probably not a good candidate for high velocity IR dome applications. The reported optical and hardness properties may make this appropriate for a low velocity 8-12 micron window application where rain erosion is a concern.

5.0 REFERENCES

1. Personal Communication, R. Gentilman to J. R. Koenig, 1984

2. Koenig, J. R., Presentation to AMRAAM JSPO, 1980

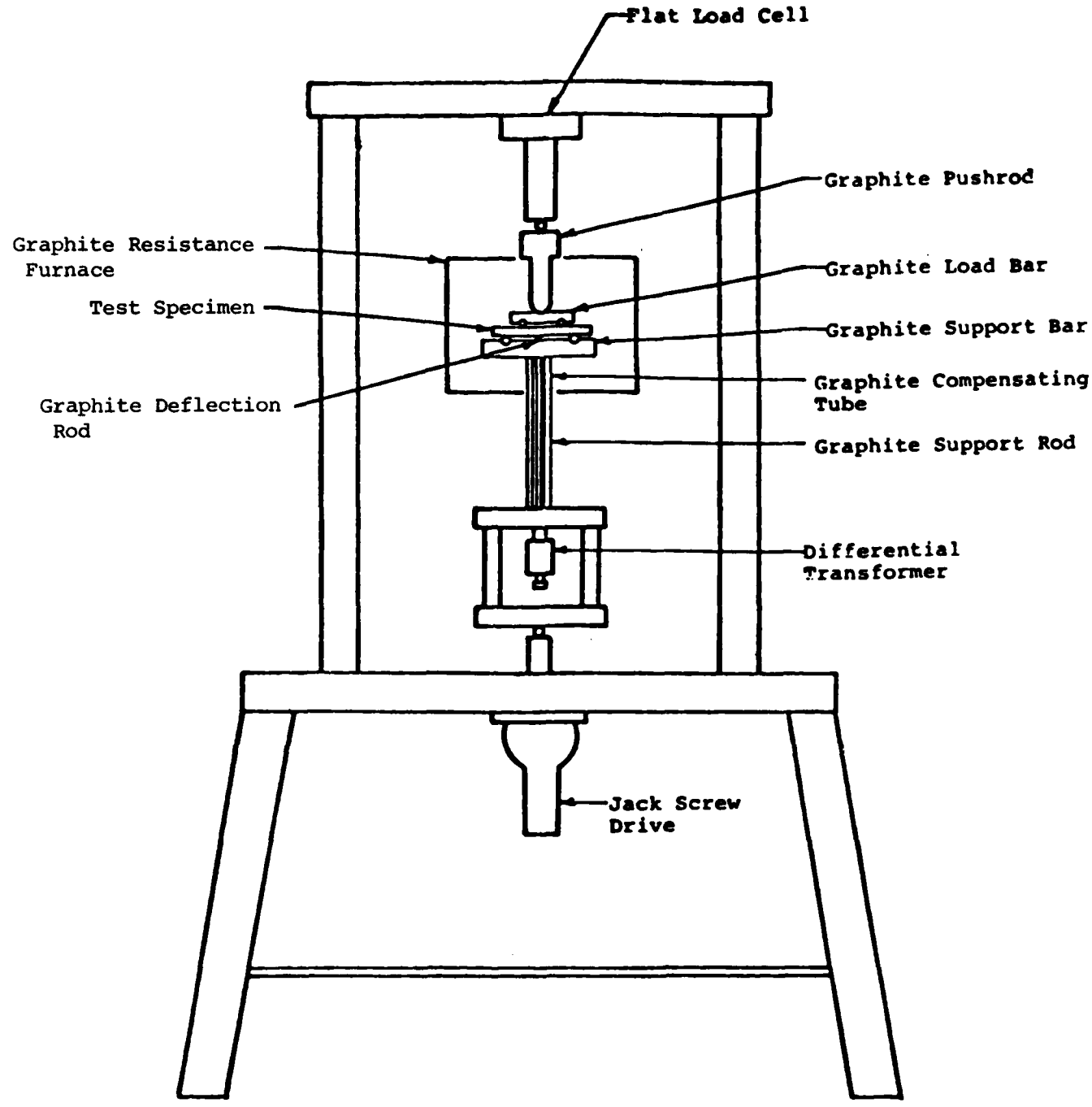

Figure 1. Schematic of High Temperature Flexural Apparatus

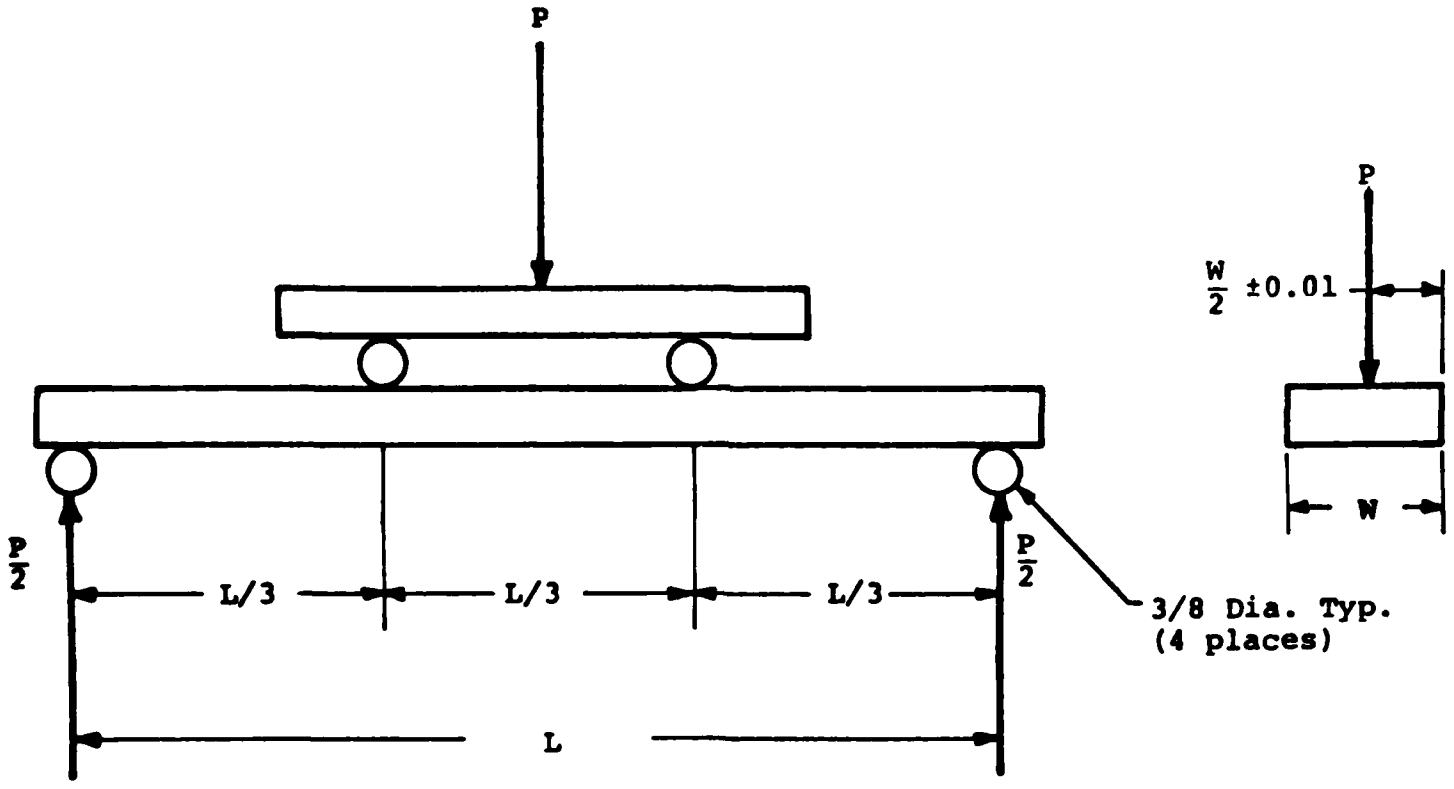

Figure 2. Flexural Four-Point Loading Set-Up

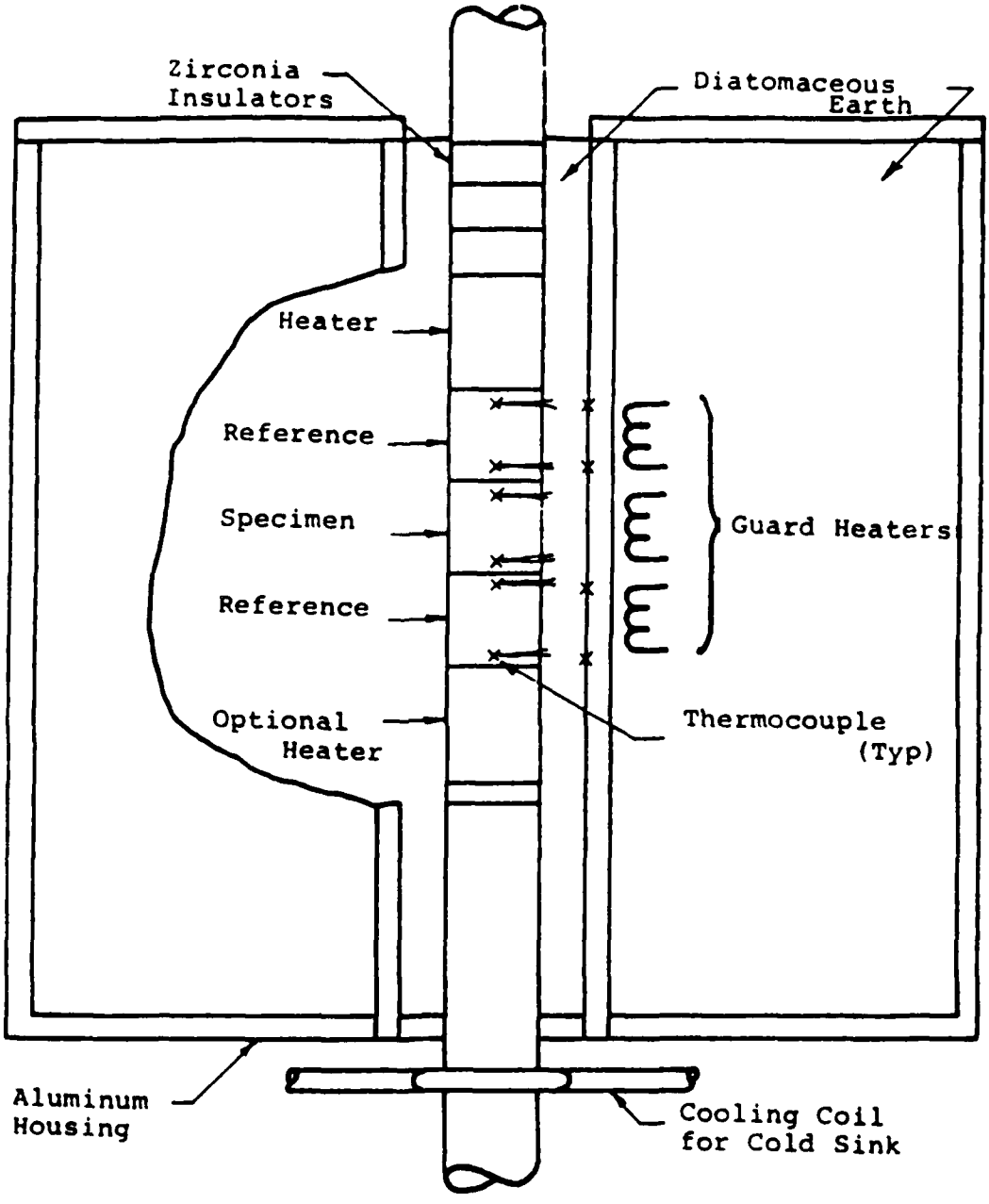

Figure 3. Schematic of Comparative Rod Thermal Conductivity Apparatus

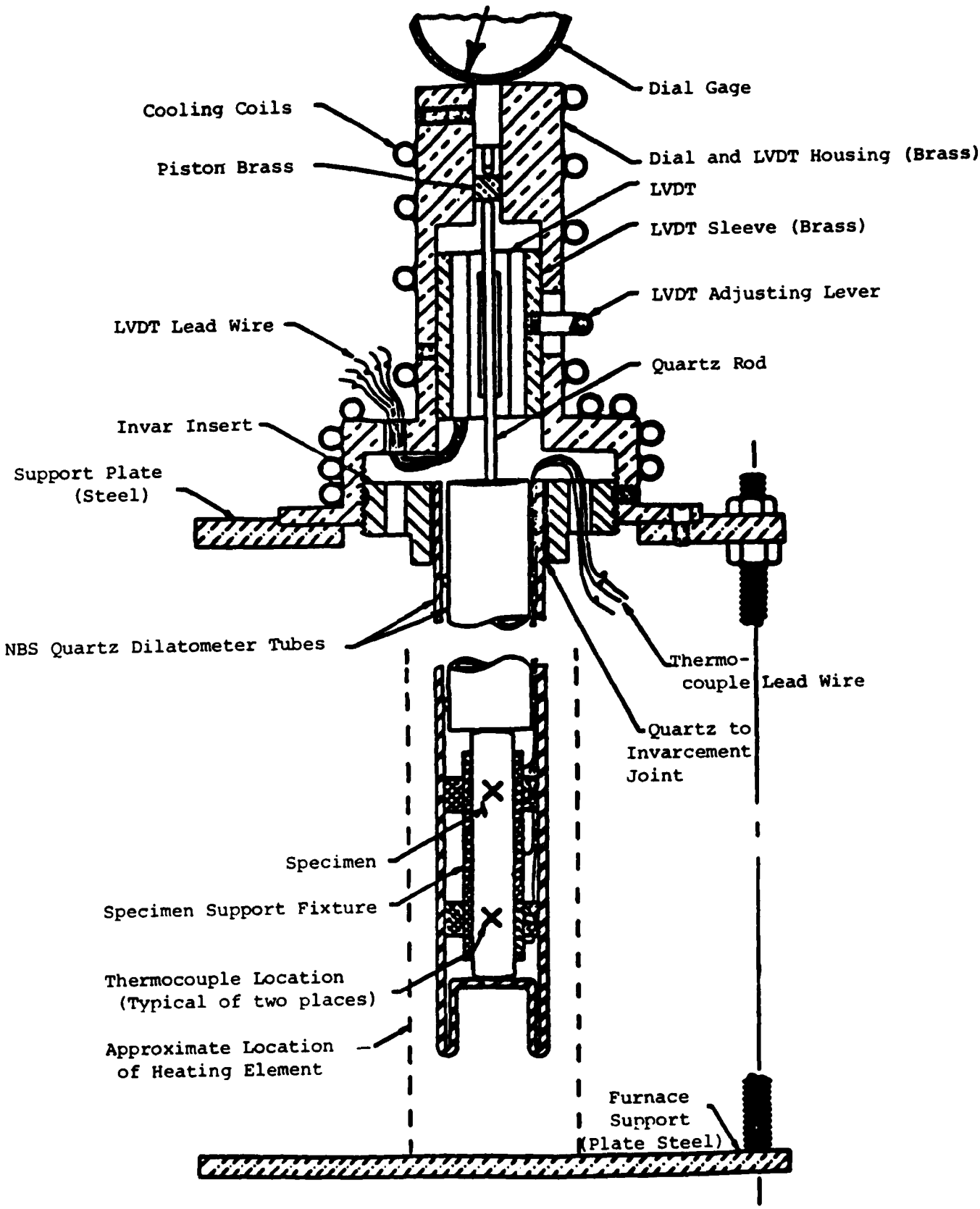

Figure 4. Assembly of Quartz Tube Dilatometer for Thermal Expansion Measurements

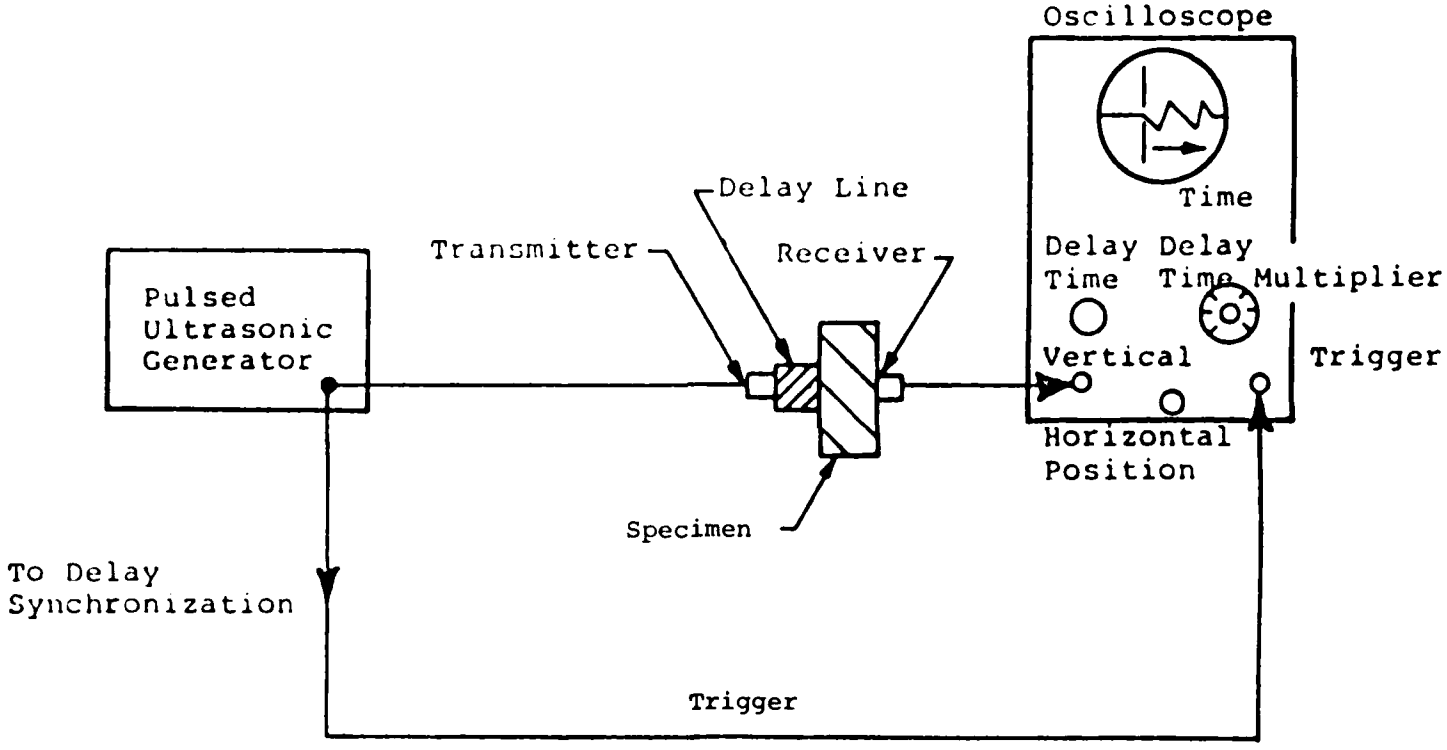

Figure 5. Block Diagram of Ultrasonic Velocity Measuring Apparatus

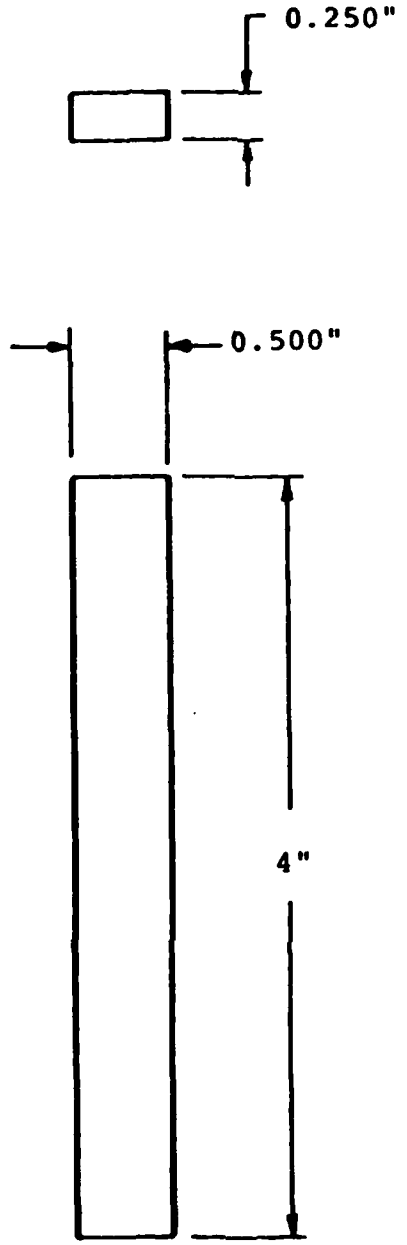

Notes: 1. Break corners on all edges

2. Surfaces to be ground parallel to length

Figure 6. Flexural Specimen Configuration

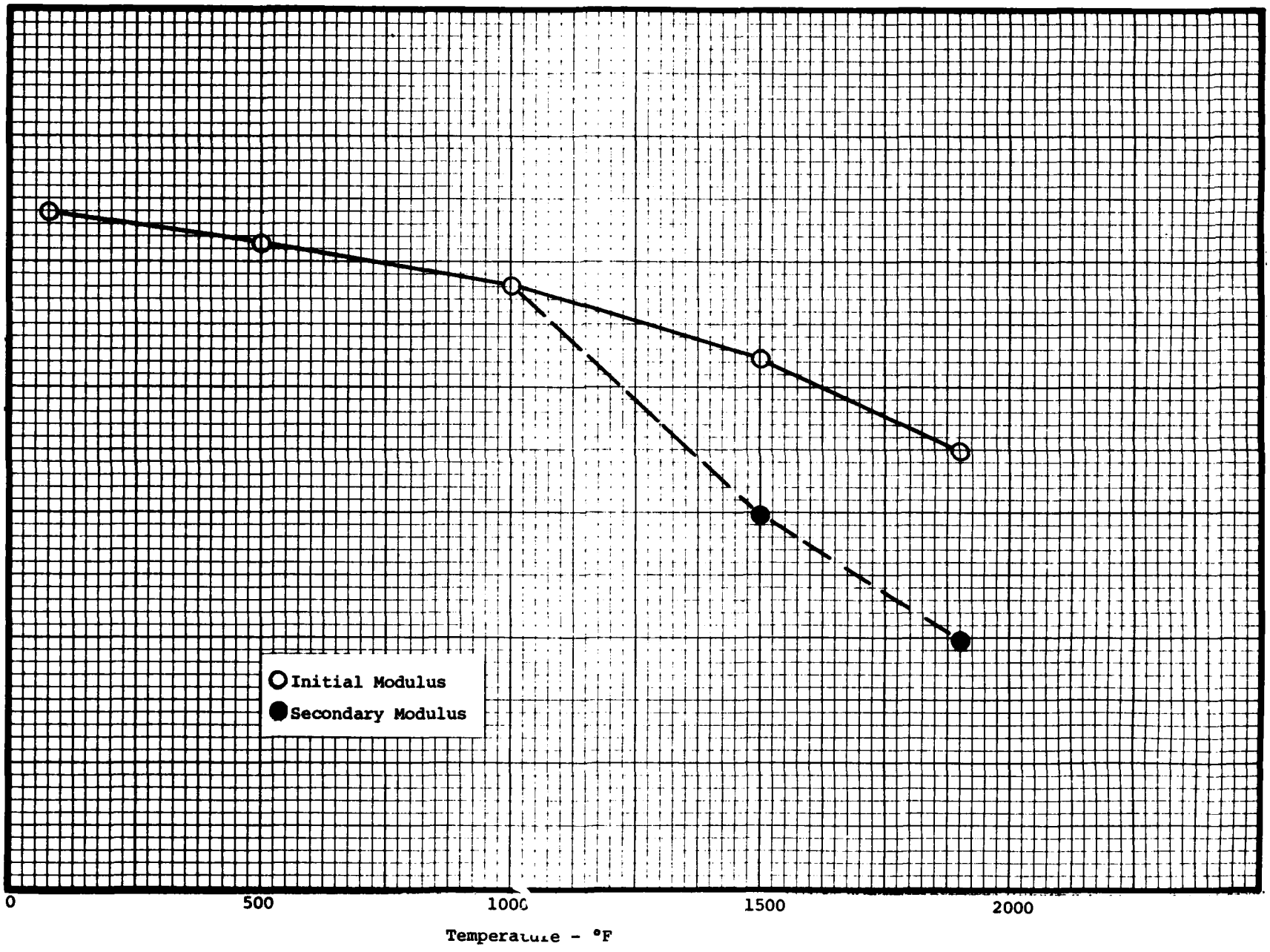

Figure 7. Flexural Moduli of $CaLa_2S_4$ as a Function of Temperature

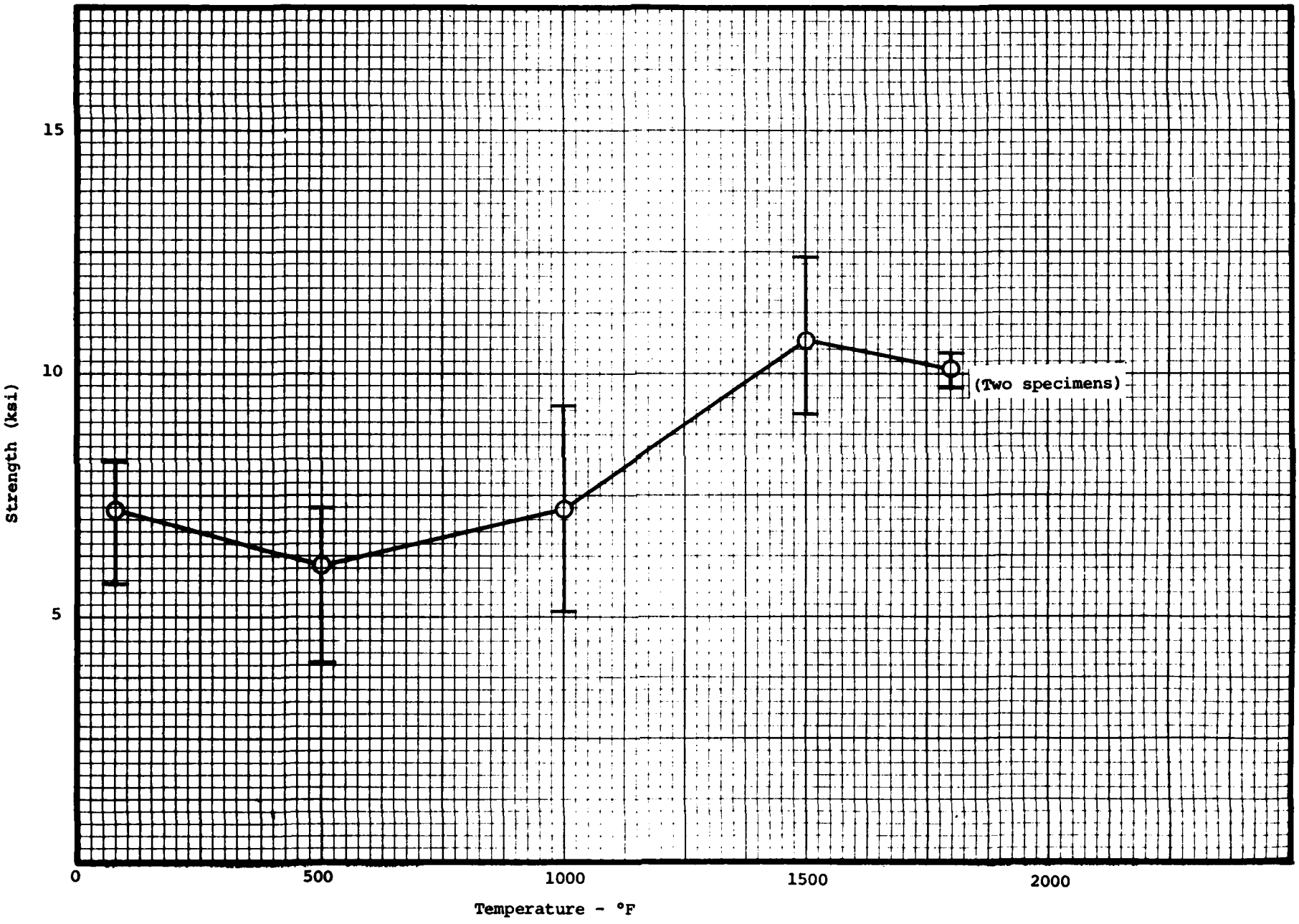

Figure 8. Strength versus Temperature for $CaLa_2S_4$

Figure 9. EDS Scan of $CaLa_2S_4$ Specimen Fracture Face

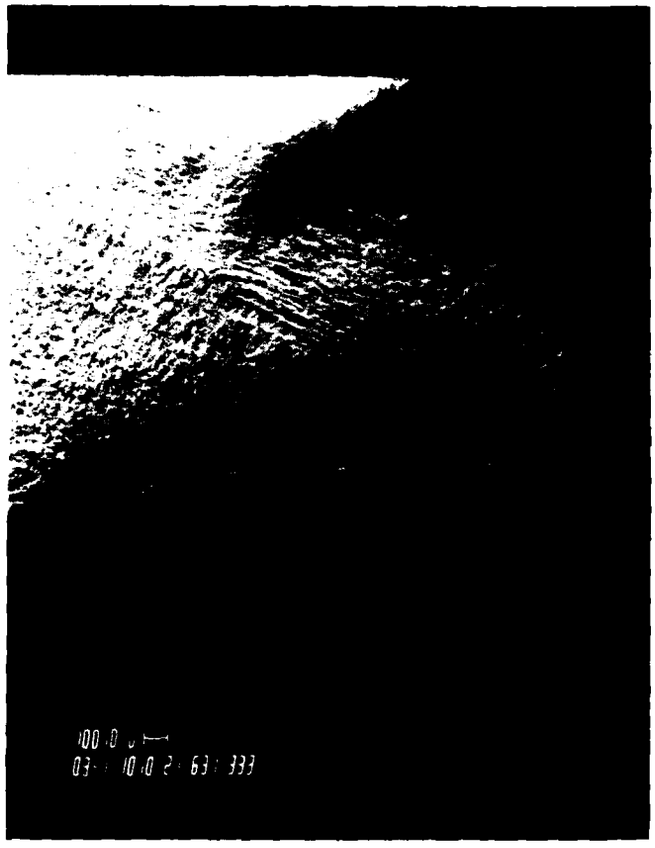

Figure 10. Failure Surface of F-10

Figure 11. Probable Initiation Site in F-10

Figure 12. Higher Magnification of Probable Initiation Site in F-10

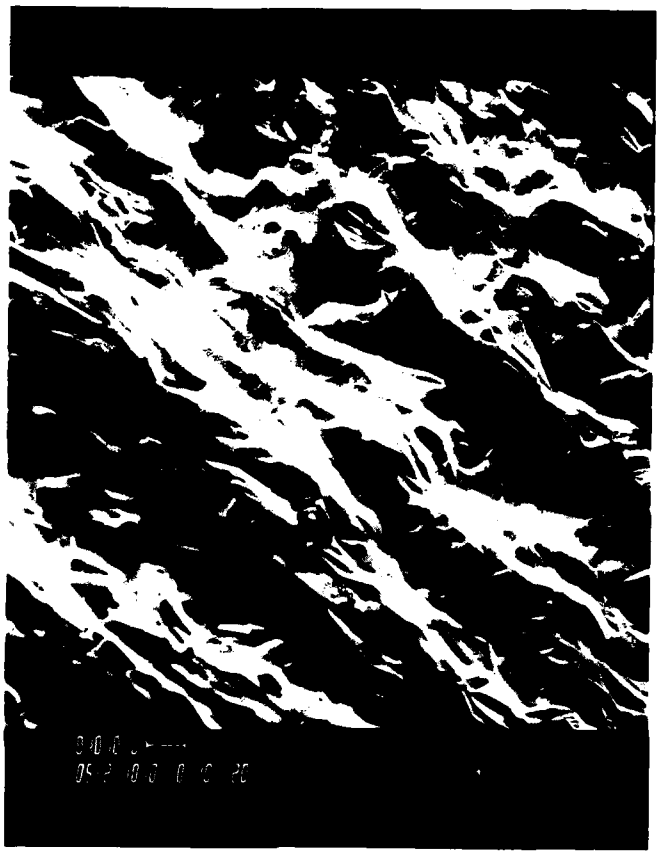

Figure 13. Structure in "Hackle" seen in Figure 10.

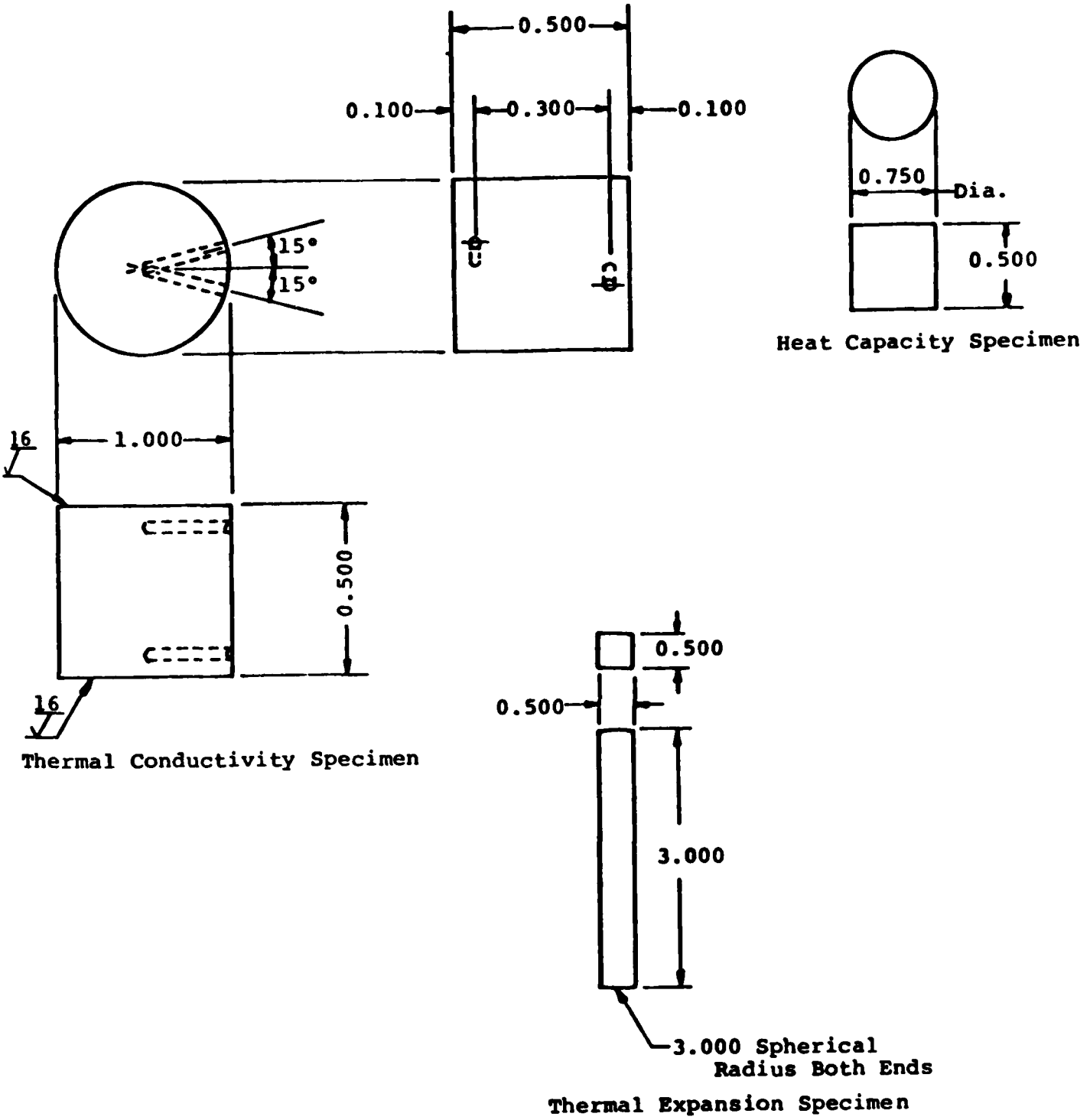

Figure 14. Thermal Specimen Configurations

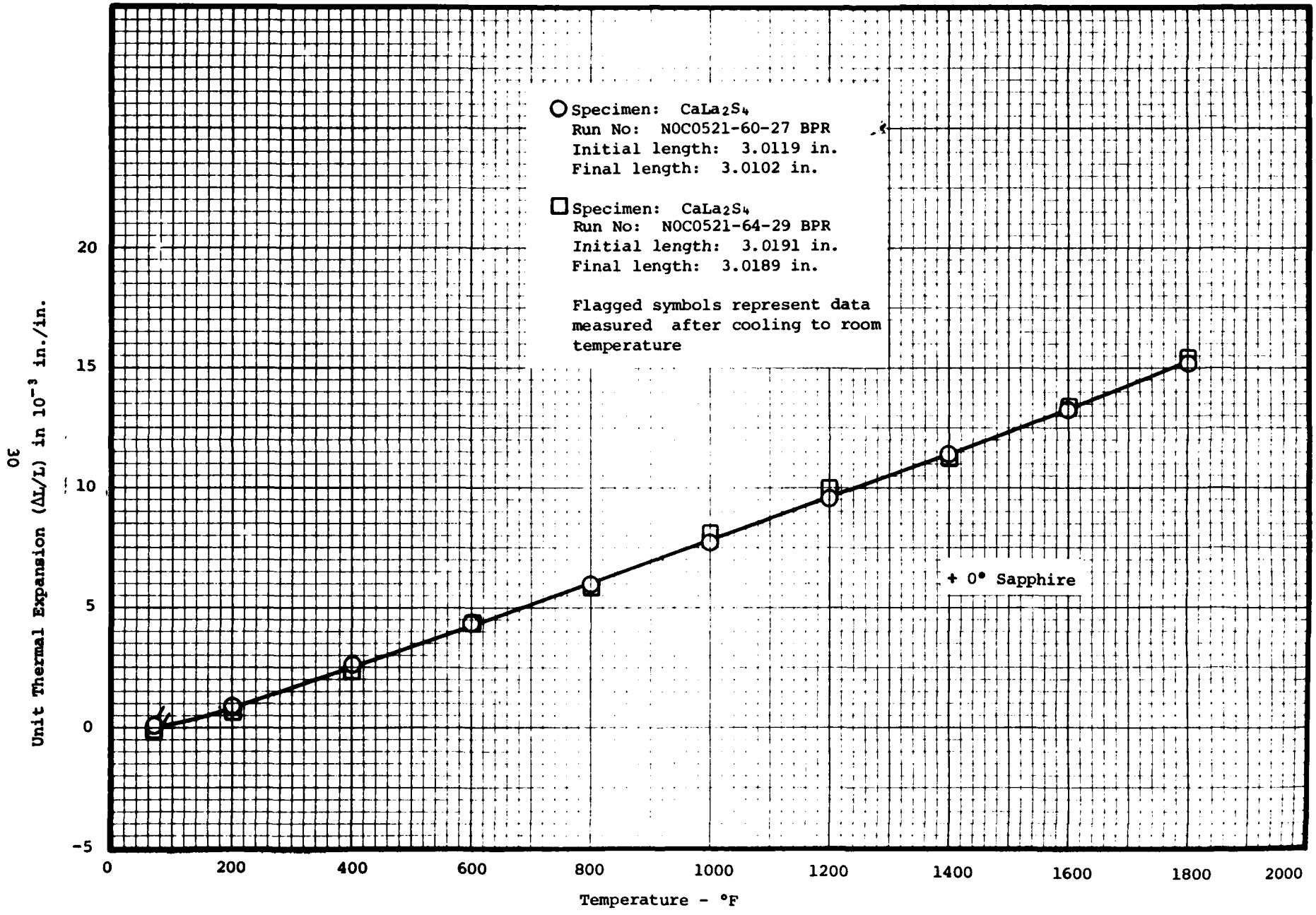

Figure 15. Thermal Expansion of $CaLa_2S_4$

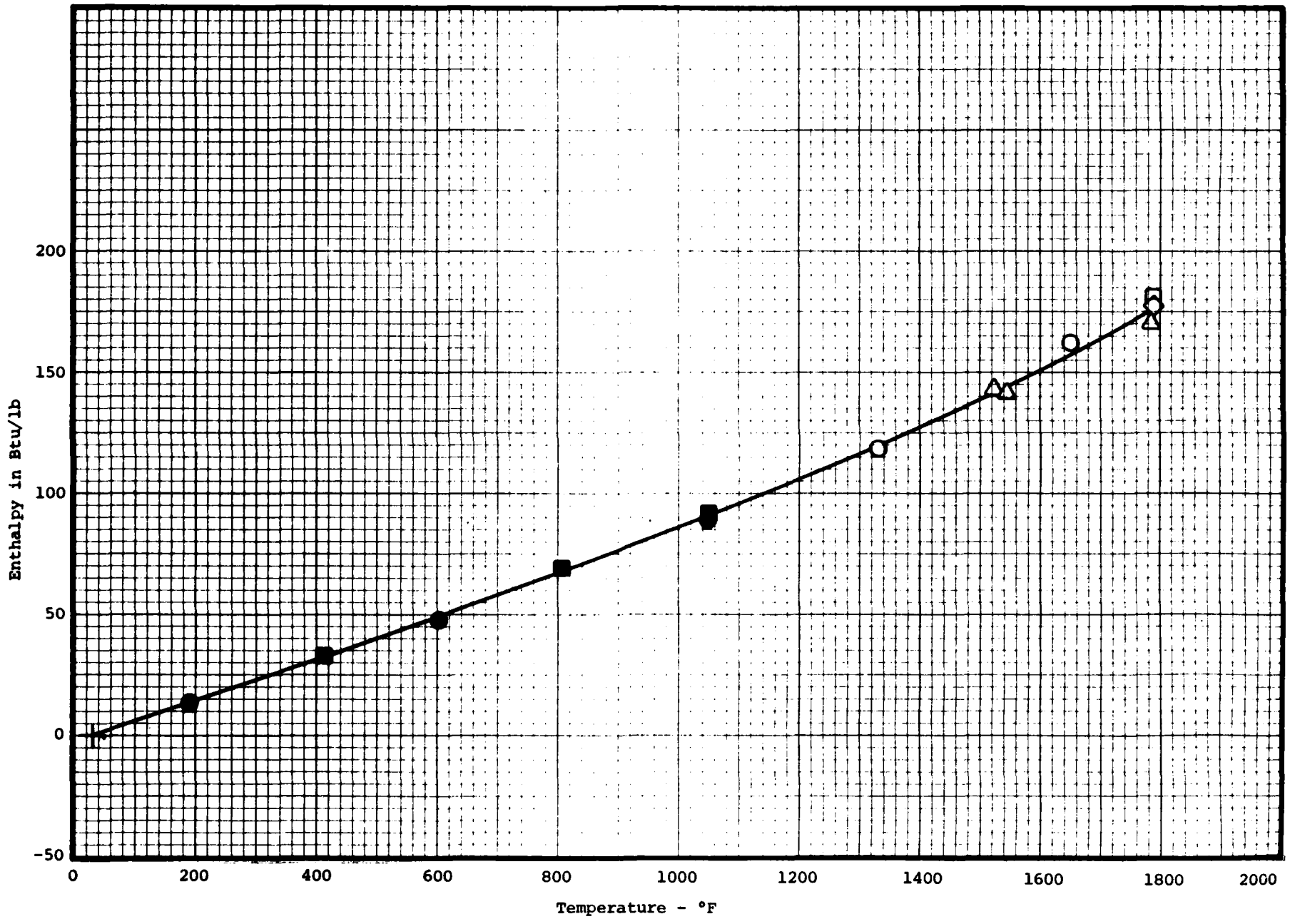

Figure 16. Enthalpy Plot for $CaLa_2S_4$

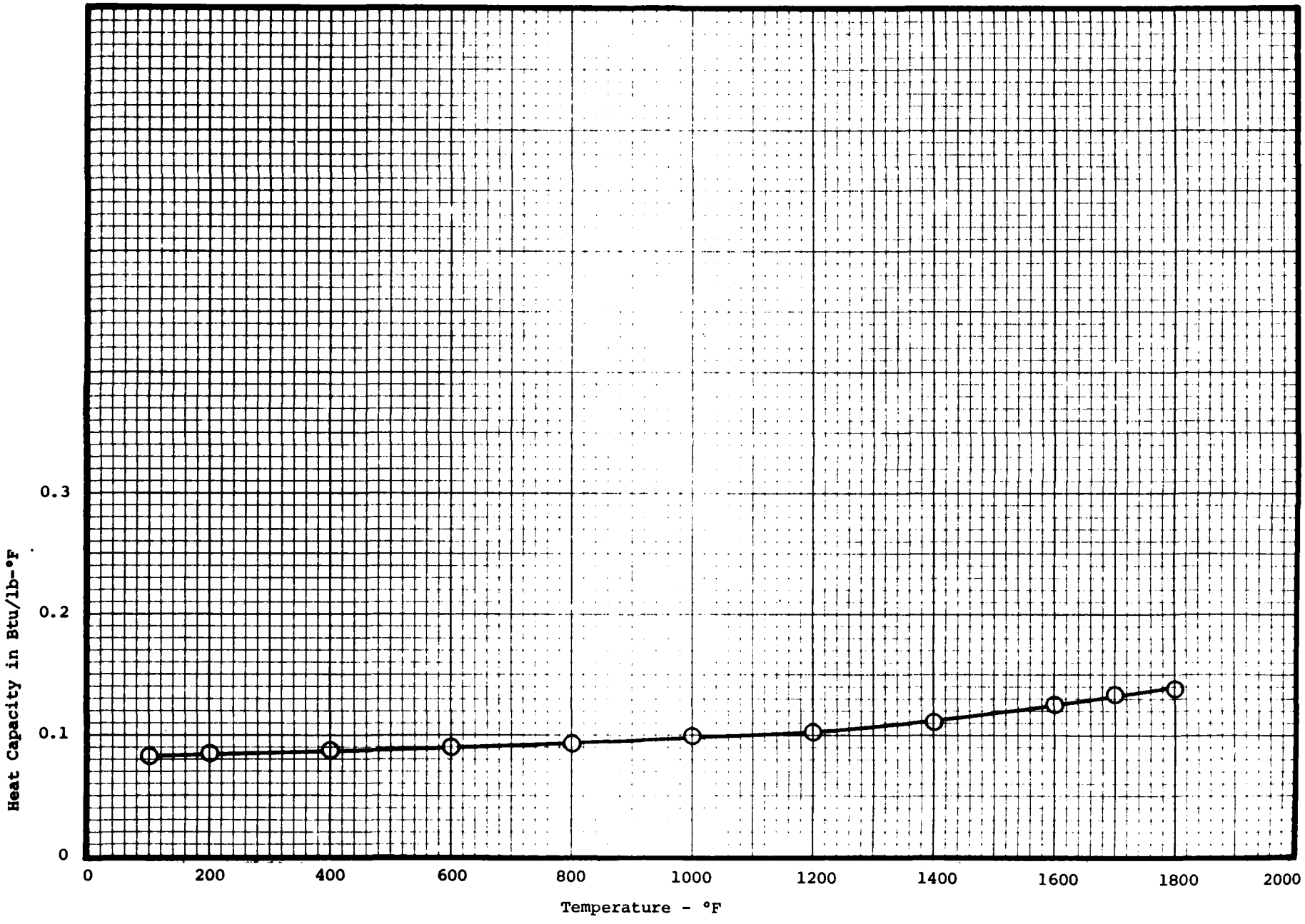

Figure 17. Specific Heat of $CaLa_2S_4$

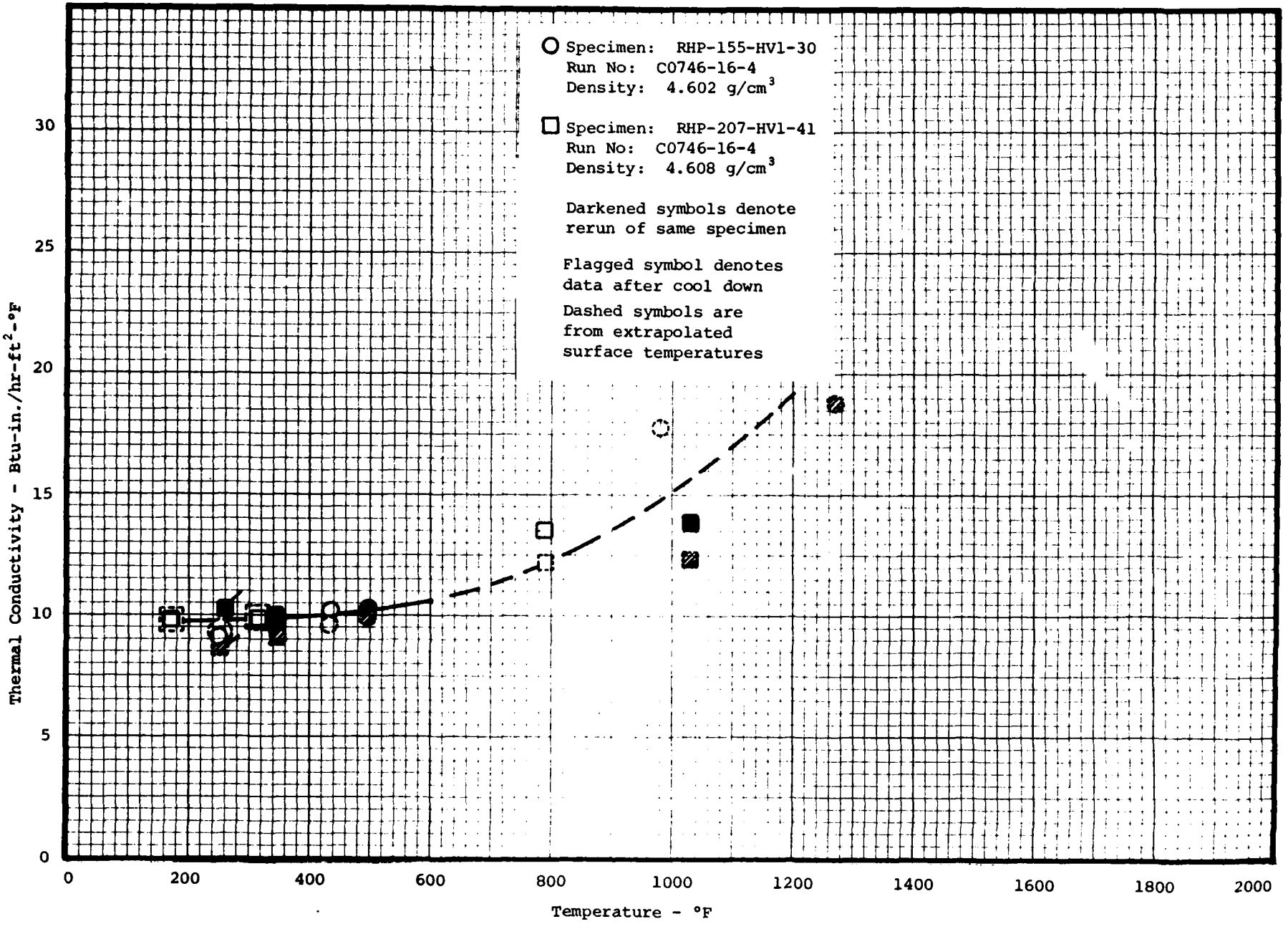

Figure 18. Thermal Conductivity of $CaLa_2S_4$

Table 1. Test Matrix for $CaLa_2S_4$

	Temperature °F				
	70	500	1000	1500	1800
Flexural Strength and Modulus	5	4	4	4	2
Thermal Expansion	2 →				
Specific Heat	2 →				
Thermal Conductivity	2 →				
Density	X				
Sonic Velocity	X				

Table 2. Density and Velocity of $CaLa_2S_4$ Specimens

Specimen Number	Density (gm/cc)	Velocity (in./μsec)	ρv^2 (10^6 psi)
RHP-145-HV1-26 #22 (TE)	4.591	0.201	17.46
RHP-220-HVI-47 #31 (TE)	4.558	0.201	17.33
RHP-155-HVI-30 #22-1 (TC)	4.591	0.204	18.05
RHP-207-HVI-41 #32 (TC)	4.608	0.202	17.69
RHP-155-HVI-30 #22-2 (SH)	4.604	0.202	17.68
RHP-155-HVI-30 #29 (SH)	4.609	0.204	18.05
F-1	4.616	0.201	17.55
F-2	4.631	0.201	17.61
F-3	4.632	0.201	17.62
F-4	4.643	0.201	17.66
F-5	4.641	0.201	17.65
F-6			
F-7	4.621	0.201	17.66
F-8	4.621	0.201	17.66
F-9	4.619	0.201	17.57
F-10	4.619	0.201	17.57
F-11	4.611	0.201	17.54
F-12	4.619	0.201	17.57
F-13	4.608	0.201	17.52
F-14	4.610	0.201	17.53
F-15	4.618	0.201	17.39
F-16	4.603	0.201	17.50
F-17	4.597	0.201	17.48
F-18			
F-19	4.603	0.201	17.50
F-20	4.588	0.200	17.27
F-21	4.602	0.200	17.33
F-23	4.586	0.201	17.44

Table 3. Flexural Properties of $CaLa_2S_4$ IR Window Material

Specimen Number	Temp (°F)	Density (g/cm^3)	Strength (ksi)	Ultimate Deflection (in.)	Flexural Modulus (Msi) E_{Init} (70 °F)	E_{Init} (Test)	E_{II} (Test)	Bilinear Yield Point (in.)
1	70	4.616	7.97	0.0086	13.88	14.05	-	-
5	70	4.641	5.67	0.0064	13.48	13.44	-	-
10	70	4.619	6.45	0.0073	12.71	13.29	-	-
14	70	4.610	8.20	0.0091	13.75	13.78	-	-
19	70	4.603	7.89	0.0092	13.89	13.30	-	-
Average		4.618	7.24	0.0081	13.54	13.57		
Std. Deviation			1.11	0.0012	0.49	0.33		
2	500	4.631	7.24	0.0085	13.21	12.88	-	-
11	500	4.611	6.62	0.0079	13.44	12.81	-	-
12	500	4.619	6.39	0.0077	13.05	12.51	-	-
15	500	4.618	4.05	0.0047	14.34	13.36	-	-
Average		4.620	6.08	0.0072	13.51	12.89		
Std. Deviation			1.40	0.0017	0.58	0.35		
3	1000	4.632	5.11	0.0068	13.48	11.70	-	-
7	1000	4.645	6.23	0.0077	14.30	12.48	-	-
9	1000	4.621	8.23	0.0104	13.47	11.96	-	-
13	1000	4.608	9.34	0.0120	13.46	11.99	-	-
Average		4.627	7.23	0.0092	13.68	12.03		
Std. Deviation			1.91	0.0024	0.42	0.33		
4	1500	4.643	12.40	0.0237	13.47	10.30	7.15	0.0068
8	1500	4.643	9.20	0.0164	12.71	10.69	7.98	0.0044
17	1500	4.597	9.35	0.0164	13.58	10.53	7.57	0.0071
23	1500	4.586	11.85	0.0212	13.41	10.78	7.13	0.0080
Average		4.617	10.70	0.0194	13.29	10.56	7.46	0.0066
Std. Deviation			1.67	0.0036	0.39	0.21	0.40	0.0015
20	1800	4.588	10.40	0.0307	13.34	7.95	4.58	0.0081
21	1800	4.602	9.71	0.0251	13.15	9.53	5.30	0.0052
Average		4.595	10.06	0.0279	13.25	8.74	4.94	0.0067

Table 4. Thermal Expansion of $CaLa_2S_4$ - Encl 4 Measured in Quartz Dilatometer

Specimen	Time	Specimen Temperatures - °F Top	Bottom	Average	Observed Total Elongation 10^{-3} in.	Observed Unit Elongation 10^{-3} in./in.	Unit Elongation Correction for Dilatometer Motion 10^{-3} in./in.	Corrected Specimen Unit Elongation 10^{-3} in./in.
RHP-220, HVI-47-31 $CaLa_2S_4$- Encl-4 Run: N0C0521-60-27 BPR				Initial length: 3.0119 in. Final length: 3.0102 in.			Initial weight: 60.2514 gm Final weight: 60.2498 gm	
	9:08	70	70	70	0.0	0.0	0.0	0.0
	9:25	200	200	200	2.40	0.80	0.05	0.85
	9:40	400	400	400	7.48	2.48	0.12	2.60
	9:55	600	600	600	12.47	4.14	0.19	4.33
	10:10	800	800	800	17.30	5.74	0.25	5.99
	10:18	1000	1000	1000	22.30	7.40	0.30	7.70
	10:28	1200	1200	1200	27.78	9.22	0.35	9.57
	10:40	1400	1400	1400	33.20	11.02	0.41	11.43
	10:51	1600	1600	1600	38.50	12.78	0.46	13.24
	11:11	1800	1800	1800	44.20	14.68	0.52	15.20
	7:45	70	70	70	0.10	0.03	0.0	0.03

Table 5. Thermal Expansion of $CaLa_2S_4$ - Encl 4 Measured in Quartz Dilatometer

Specimen	Time	Specimen Temperatures - °F Top	Bottom	Average	Observed Total Elongation 10^{-3} in.	Observed Unit Elongation 10^{-3} in./in.	Unit Elongation Correction for Dilatometer Motion 10^{-3} in./in.	Corrected Specimen Unit Elongation 10^{-3} in./in.
RHP-145, HV1-26 #22								
$CaLa_2S_4$ - Encl 4				Initial length: 3.0191 in.			Initial weight: 52.2260 gm	
Run: NOC0521-64-29 BPR				Final length: 3.0189 in.			Final weight: 52.2237 gm	
	8:45	70	70	70	0.0	0.0	0.0	0.0
	9:00	200	200	200	1.70	0.56	0.05	0.61
	9:18	400	400	400	6.97	2.31	0.11	2.42
	9:34	600	600	600	12.63	4.18	0.17	4.35
	9:45	800	800	800	17.07	5.65	0.23	5.88
	9:57	1000	1000	1000	23.57	7.81	0.32	8.13
	10:10	1200	1200	1200	29.07	9.63	0.39	10.02
	10:20	1400	1400	1400	32.47	10.75	0.48	11.23
	10:30	1600	1600	1600	38.67	12.81	0.57	13.38
	10:47	1800	1800	1800	44.39	14.70	0.65	15.35
	8:00	70	70	70	- 0.11	- 0.04	0.0	- 0.04

Table 6. Enthalpy of $CaLa_2S_4$ Measured in the Adiabatic Calorimeter

Specimen	Run	Initial Cup Temp °F	Final Cup Temp °F	Change in Cup Temp °F	Initial Sample Temp °F	Initial Weight of Sample gm	Final Weight of Sample gm	Enthalpy $h = \frac{K}{W_s}(t_2-t_1)$ Btu/lb	Enthalpy Btu/lb Above 85 °F Ref.	Enthalpy Btu/lb Above 32 °F Ref
	NOC0215-									
HC-22-2	120	71.364	75.364	4.000	413	16.2762	16.2710	29.60	28.76	33.40
	121	72.465	81.261	8.796	807	16.2710	16.2475	65.17	64.84	69.60
	122	78.839	90.348	11.509	1059	16.2475	15.9695	86.76	87.23	91.98
HC-29-2	120	72.248	78.174	5.926	602	16.1804	16.1824	44.02	43.45	47.90
	119	73.364	74.739	1.375	193	16.1926	16.1887	10.28	9.34	13.93
	121	80.682	91.913	11.23	1051	16.1824	16.1305	83.81	84.41	89.05

Table 8. Thermal Conductivity of $CaLa_2S_4$ - Encl 6 using Comparative Rod Apparatus with TM-Silica References

Specimen and Time	Mean Temperature of Specimen °F	Thermal Conductivity of Specimen - k_s Btu-in./hr-ft^2-°F	ΔT through Specimen °F	Heat Flux through Specimen Btu/hr-ft^2	Heat Flux through Upper Reference Btu/hr-ft^2	Heat Flux through Middle Reference Btu/hr-ft^2	Heat Flux through Lower Reference Btu/hr-ft^2
RHP-155-HV1-30 #22-1							
Run: NOC0746-16-4							
Run: 1			Initial thickness: 0.5050 in.			Initial weight: 29.7989 gm	
Density: 4.602 g/cm^3			Final thickness: 0.5053 in.			Final weight: 29.7425 gm	
8/20/84							
2:00 P.M.	249	9.09	19.00	566	639	534	596
2:30	249	9.07	19.00	565	639	533	596
8/21/85							
5:10 A.M.	433	10.23	26.63	893	1003	846	935
5:40	433	10.29	26.64	899	1004	854	934

Table 9. Thermal Conductivity of $CaLa_2S_4$ - Encl 6 using Comparative Rod Apparatus with TM-Silica References

Specimen and Time	Mean Temperature of Specimen °F	Thermal Conductivity of Specimen - ks Btu-in./hr-ft^2-°F	ΔT through Specimen °F	Heat Flux through Specimen Btu/hr-ft^2	Heat Flux through Upper Reference Btu/hr-ft^2	Heat Flux through Middle Reference Btu/hr-ft^2	Heat Flux through Lower Reference Btu/hr-ft^2
RHP-207-HV1-41 #32 Run: NOC0746-16-4 Run: 1 Density: 4.608 g/cm^3			Initial thickness: 0.5058 in. Final thickness: 0.5057 in.		Initial weight: 29.7898 gm Final weight: 29.7837 gm		
8/20/84							
2:00 P.M.	169	9.77	16.99	543	639	534	596
2:30	169	9.73	17.03	542	639	533	596
8/21/85							
5:10 A.M.	316	9.82	26.74	859	1003	846	935
5:40	316	9.90	26.75	866	1004	854	934
10:45	787	13.49	39.17	1728	1988	1687	1962
11:15	788	13.57	39.13	1736	1989	1696	1963

Table 10. Thermal Conductivity of $CaLa_2S_4$ - Encl 6 using Comparative Rod Apparatus with TM-Silica References

Specimen and Time	Mean Temperature of Specimen °F	Thermal Conductivity of Specimen - k_s Btu-in./hr-ft^2-°F	ΔT through Specimen °F	Heat Flux through Specimen Btu/hr-ft^2	Heat Flux through Upper Reference Btu/hr-ft^2	Heat Flux through Middle Reference Btu/hr-ft^2	Heat Flux through Lower Reference Btu/hr-ft^2
RHP-155-HV1-30 #22-1							
Run: NOC0746-19-4							
Run: 2			Initial thickness: 0.5053 in.			Initial weight: 29.7425 gm	
Density: 4.570 g/cm^3			Final thickness: 0.5054 in.			Final weight: 29.7222 gm	
8/28/84							
9:30 A.M.	497	10.25	35.42	1191	1355	1121	1288
10:00	497	10.28	35.40	1192	1356	1121	1290

Table 11. Thermal Conductivity of $CaLa_2S_4$ - Encl 6 using Comparative Rod Apparatus with TM-Silica References

Specimen and Time	Mean Temperature of Specimen °F	Thermal Conductivity of Specimen - k_s Btu-in./hr-ft^2-°F	ΔT through Specimen °F	Heat Flux through Specimen Btu/hr-ft^2	Heat Flux through Upper Reference Btu/hr-ft^2	Heat Flux through Middle Reference Btu/hr-ft^2	Heat Flux through Lower Reference Btu/hr-ft^2
RHP-207-HV1-41 #32 Run: NOC0746-19-4 Run: 2 Density: 4.603 g/cm^3			Initial thickness: 0.5057 in. Final thickness: 0.5058 in.			Initial weight: 29.7837 gm Final weight: 29.7837 gm	
8/28/85							
9:30 A.M.	344	9.81	35.16	1147	1355	1121	1288
10:00	344	9.95	35.21	1146	1356	1121	1290
2:00 P.M.	1031	13.81	52.79	2384	2630	2332	2676
2:30	1033	13.82	52.75	2384	2632	2333	2676
8/29/85							
6:00 A.M.	259	10.26	21.04	706	-	692	786

Table 12. Summary of $CaLa_2S_4$ Mechanical and Thermal Data

	$CaLa_2S_4$	ZnS	ZnSe
70° Flexural Strength (psi)	7240	9300	6200
1000° Flexural Strength (psi)	7230	13600	7700
70° Flexural Modulus (10^6 psi)	13.6	10.6	10.6
1000° Flexural Modulus (10^6 psi)	13.7	6.7	7.6
Thermal Expansion to 1500 °F (in./in. x 10^{-3})	12.4	6.72	7.30
Specific Heat at 500 °F (Btu/lb-°F)	0.088	0.120	0.090
Thermal Conductivity at 500 °F (Btu-in./hr-ft^2-°F)	10.5	67	55
Density (gm/cc)	4.61	4.07	5.24
Sonic Velocity (in./μsec)	0.201	0.212	0.174

APPENDIX A

FLEXURAL LOAD - DEFLECTION CURVES

SRI Run No.: F-1 [illegible] Test: [illegible]

Date: 1-8-85 Temperature: 70°F

Material: Ca La2 54

Specimen No.: 1

Loading Direction:

Lateral Strain Direction:

Stress / ~~Strain~~ Rate: 10000 psi/min

X Scale: .1V 1" = .002

Y Scale: .5mV 1" = 13.3185 (2550)

Specimen Gage Section: 0.1980 X 0.4990 X 4.000

1.25 X 2.750 in. gage

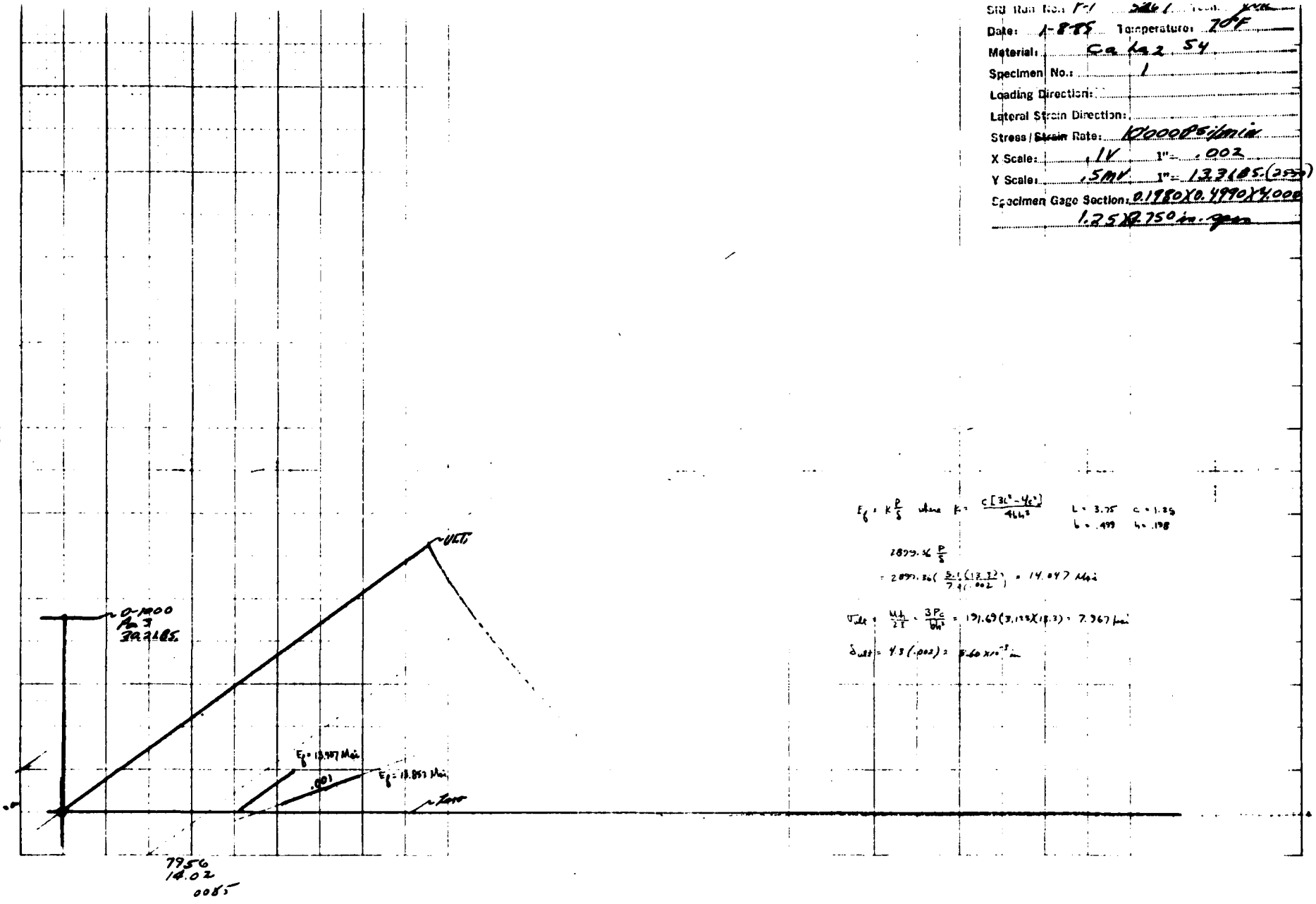

$E_f = K\frac{P}{\delta}$ where $K = \frac{c[3L^2 - 4c^2]}{4bh^2}$ $L = 3.75$ $c = 1.25$ $b = .499$ $h = .198$

$2899.36\frac{P}{\delta}$

$= 2899.36\left(\frac{5.1(13.3)}{7.4(.002)}\right) = 14.047$ Msi

$\sigma_{ult} = \frac{Mh}{2I} = \frac{3Pc}{bh^2} = 191.69(3.125)(13.3) = 7.967$ psi

$\delta_{ult} = 4.3(.002) = 5.60 \times 10^{-3}$ in

SRI Run No.: F-2 5267 Tech. York

Date: 1-8-85 Temperature: 70°F

Material: Cu La. 54

Specimen No.: 5

Loading Direction:

Lateral Strain Direction:

Stress / ~~Strain~~ Rate: 10'000 Psi/min

X Scale: .1V 1" = .002"

Y Scale: .5MV 1" = 13.3 KLBS. (2500)

Specimen Gage Section: 0.1990 X 0.500 X 4.000

1.25 X 3.75 in. Area

$\sigma_{ult} = \frac{3P_c}{bh^2} = \frac{3(2.25)(13.3)(1.25)}{(.500)(.199)^2} = 5.668$ ksi

$S_{ult} = 3.22(.004) = 6.43 \times 10^{-3}$ in/in

$E_y = 2850.22\frac{P}{\delta} = \frac{2850.2(5.6)(13.3)}{(7.9)(.002)} = 13.435$ Msi

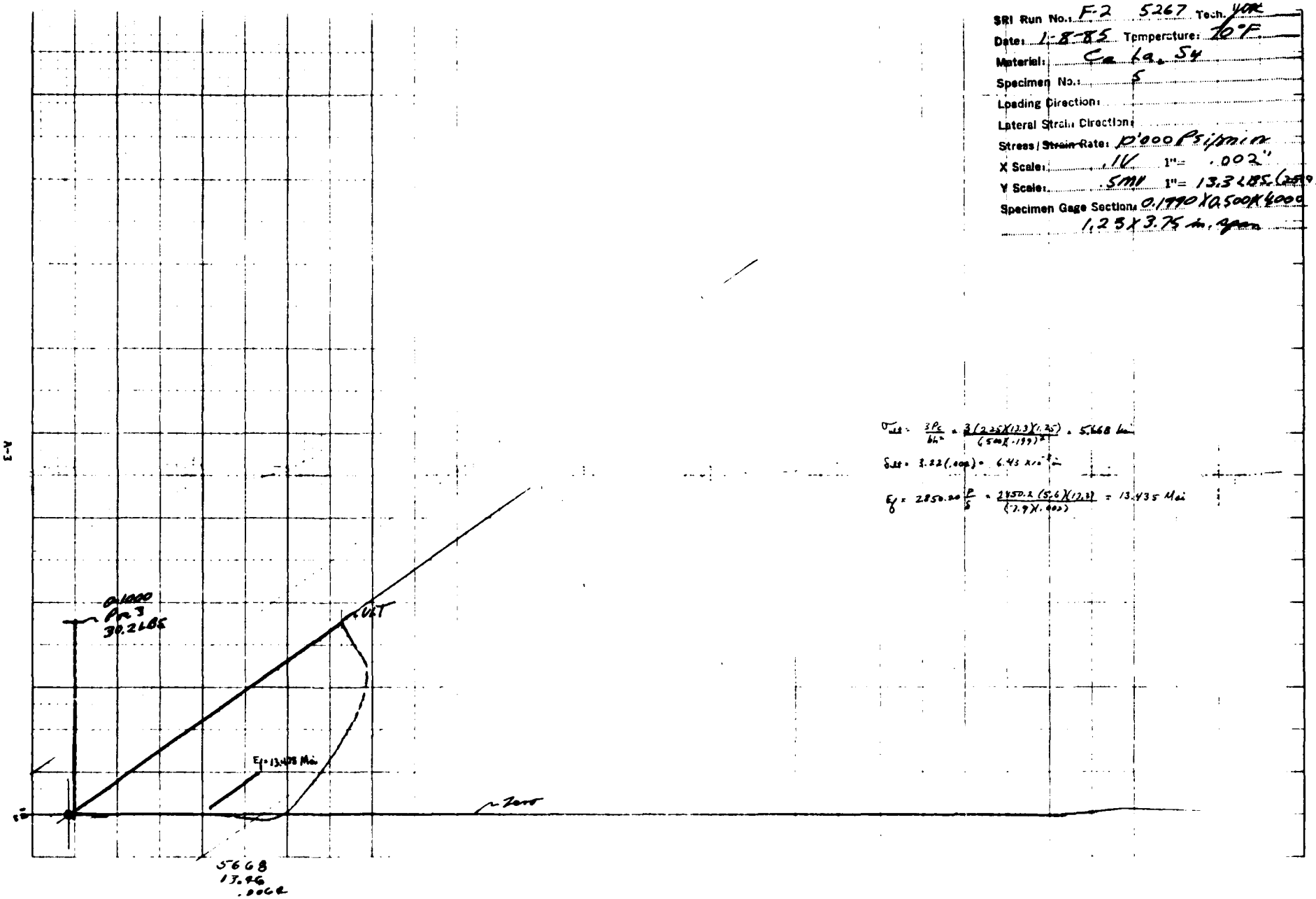

Date: 1-14-85 Temperature: 70°F

Material: Ca. Ka2 S4

Specimen No.: 10

Loading Direction:

Lateral Strain Direction:

Stress/Strain Rate: 10'000 psi/min

X Scale: .1V 1" = .002"

Y Scale: .5MV 1" = 13.3 LBS. (2547)

Specimen Gage Section: 0.2980 X 0.4995 X 4.000

1.250 in. X 3.750 in. span

Graphite load blocks

$\sigma_{ult} = \frac{3P_c}{bh^2} = \frac{3(2.53)(13.3)(1.25)}{(.4995)(.198)^2} = 6.452$ ksi

$\delta_{ult} = 3.67(.002) = 7.33 \times 10^{-3}$ in

$E_f = 2896.5 \frac{P}{\delta} = \frac{2896.5(4.9)(13.3)}{(7.1)(.002)} = 13.293$ Msi

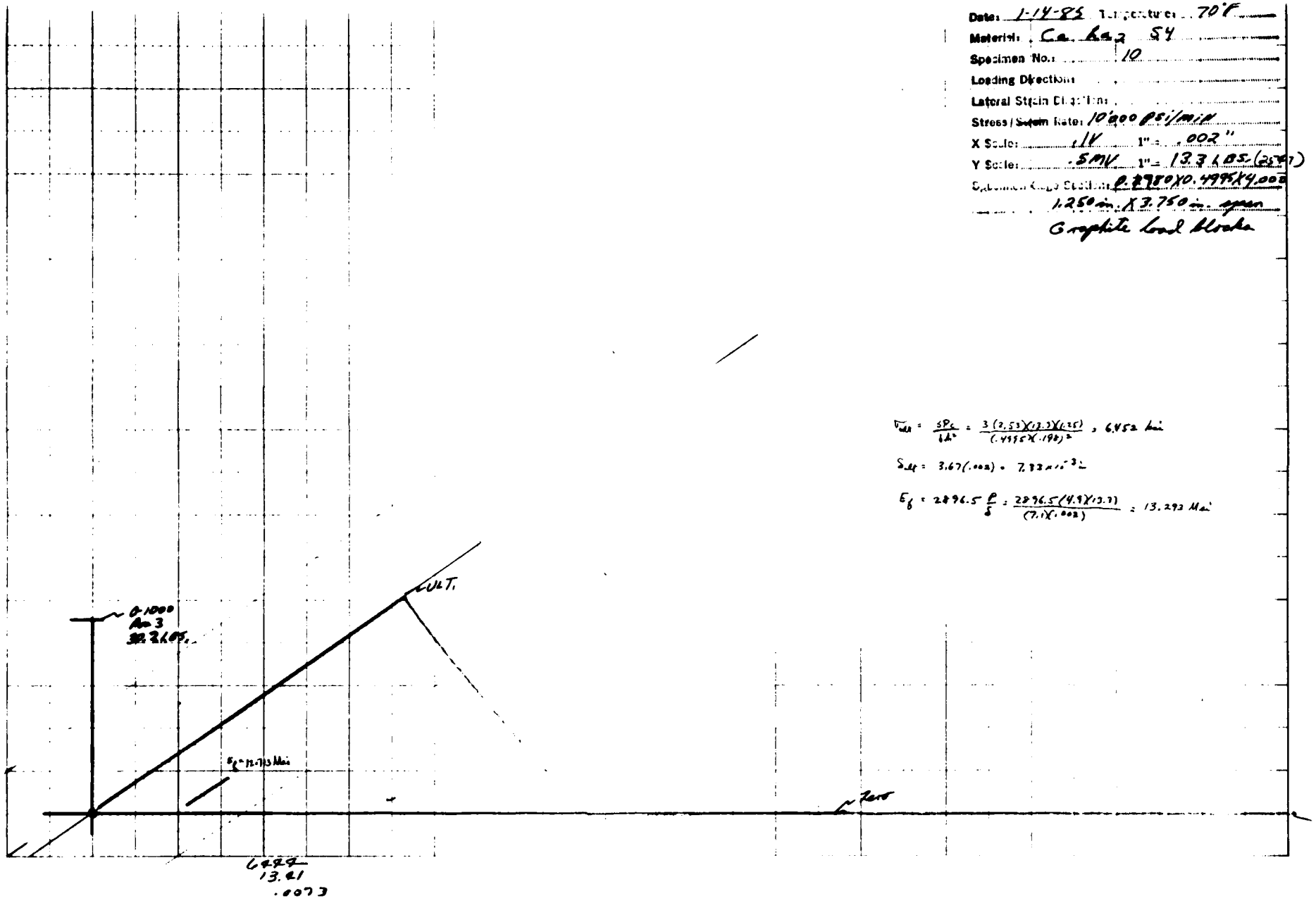

SRI Run No.: [illegible]

Date: 1-14-85 Temperature: 70°F

Material: Ca La 2 S4

Specimen No.: 14

Loading Direction:

Lateral Strain Direction:

Stress/Strain Rate: 10'000 PSI/min

X Scale: .1V 1"= .002"

Y Scale: .5mV 1"= 13.3 LBS. (2610)

Specimen Dimensions: 0.1960 X 0.4975 X 4.000

1.250 X 3.750 in. span

Graphite load Blocks

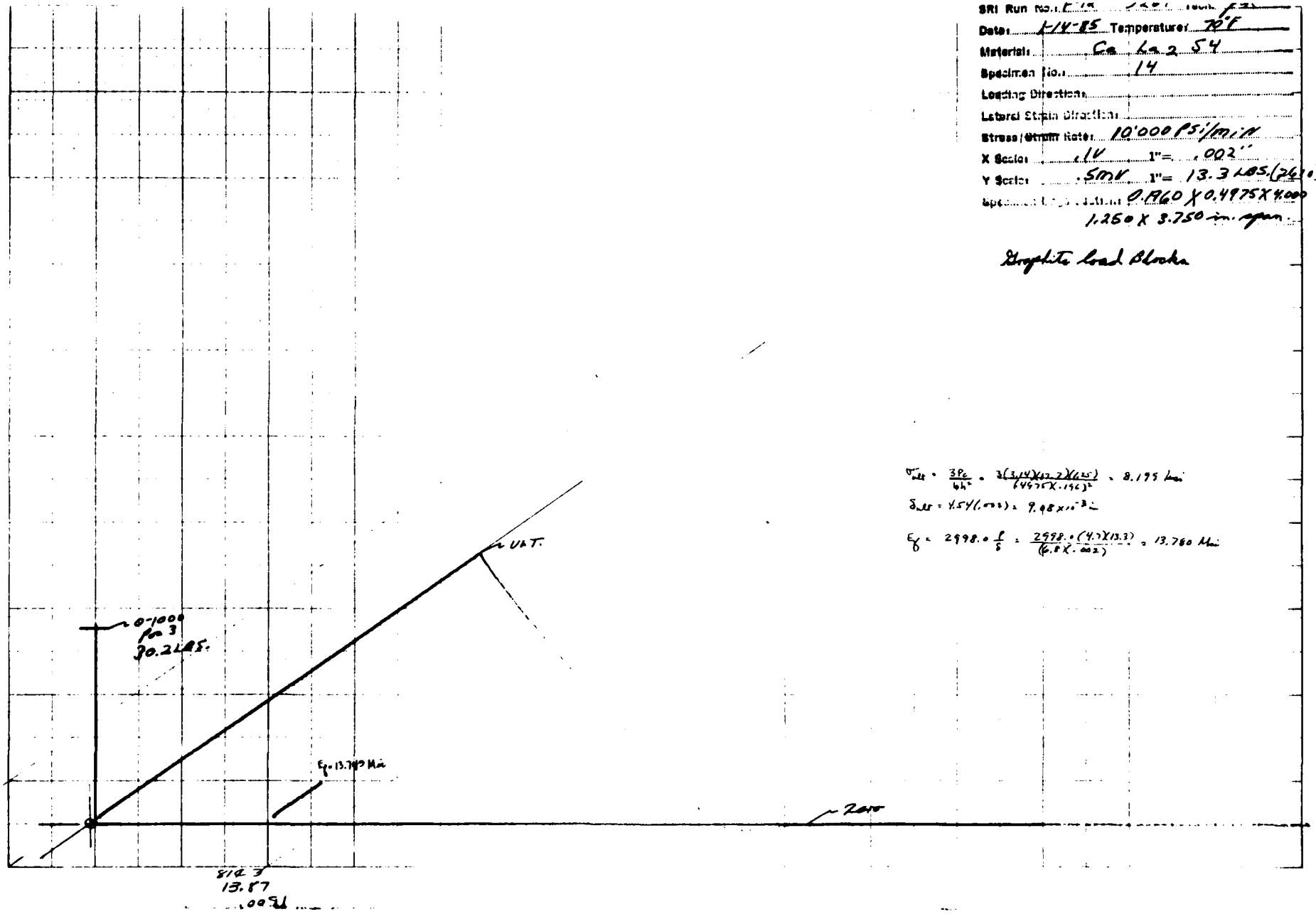

$\sigma_{ult} = \frac{3Pc}{bh^2} = \frac{3(3.14)(17.7)(1.25)}{(.4975)(.196)^2} = 8.195$ ksi

$\delta_{ult} = 4.54(.002) = 9.08 \times 10^{-3}$ in

$E_f = 2998.0 \frac{P}{\delta} = \frac{2998.0(4.7)(13.3)}{(6.8)(.002)} = 13.780$ Mai

Drill Run No.: F-13 5261 Test: yes

Date: 1-15-85 Temperature: 70°F

Material: Ca La2 S4

Specimen No.: 19

Loading Direction:

Lateral Strain Direction:

Stress/Strain Rate: 10'000 psi/min

X Scale: .1V 1" = .002"

Y Scale: .5mV 1" = 13.3685 (2559)

Specimen Gage Section: 0.1962 X 0.4995 X 4.000

1.250 X 3.750 in. span

Graphite load blocks

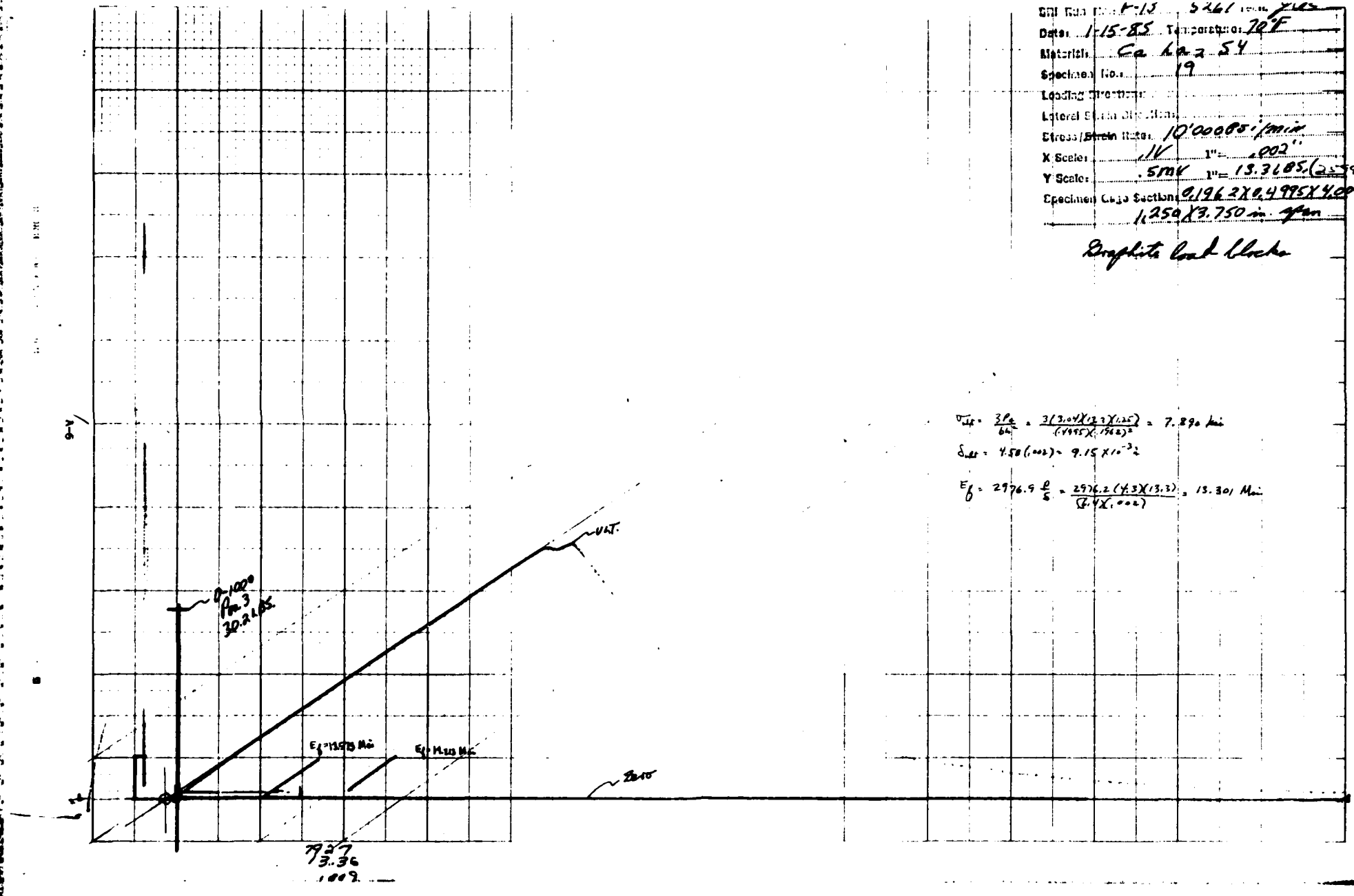

$\sigma_{ult} = \frac{3Pa}{bh^2} = \frac{3(3.04)(13.3)(1.25)}{(.4995)(.1962)^2} = 7.890$ ksi

$\delta_{ult} = 4.58(.002) = 9.15 \times 10^{-3}$ in

$E_f = 2976.9 \frac{P}{\delta} = \frac{2976.2(4.3)(13.3)}{(6.4)(.002)} = 13.301$ Msi

Stiff Run No.: F-3 3261 Tech. [illegible]

Date: 1-8-85 Temperature: 500°F

Material: Ca La2 S4

Specimen No.: 2

Loading Direction:

Lateral Strain Direction:

Stress/~~Strain~~ Rate: 10'000 psi/min

X Scale: .1V 1" = .002

Y Scale: .5MV 1" = 13.3 LBS (2550)

Specimen Gage Section: 0.1980 X 0.4992 X 4.000

1.250 X 3.750 in. span

Held 500°F for 15 min.

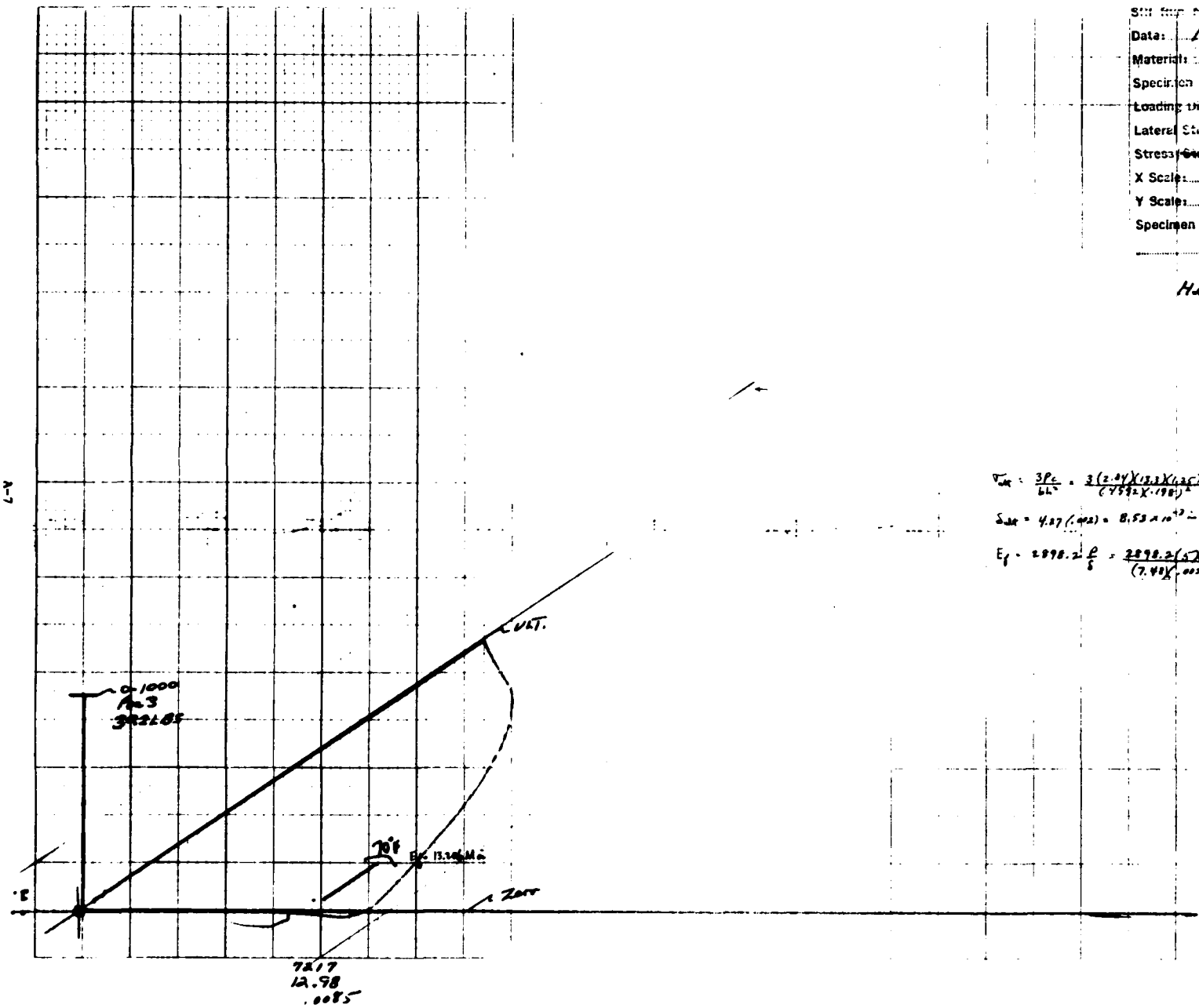

$\sigma_{ult} = \frac{3Pc}{bh^2} = \frac{3(2.84)(13.3)(1.25)}{(4992)(.198)^2} = 7.242$ ksi

$\delta_{ult} = 4.27(.002) = 8.53 \times 10^{-3}$ in

$E_f = 2898.2 \frac{P}{\delta} = \frac{2898.2(5)(13.3)}{(7.48)(.002)} = 18.877$ Mi

SRI Run No.: [illegible]

Date: 1-11-85 Temperature: 500°F

Material: Ca La2 S4

Specimen No.: 11

Loading Direction:

Lateral Strain Direction:

Stress/Strain Rate: 10'000 psi/min

X Scale: .1V 1" = .002"

Y Scale: .5mV 1" = 133 LBS. (2555)

Specimen Gage Section: 0.1978 X 0.4990 X 4.000

1.250 X 3.750 in. span

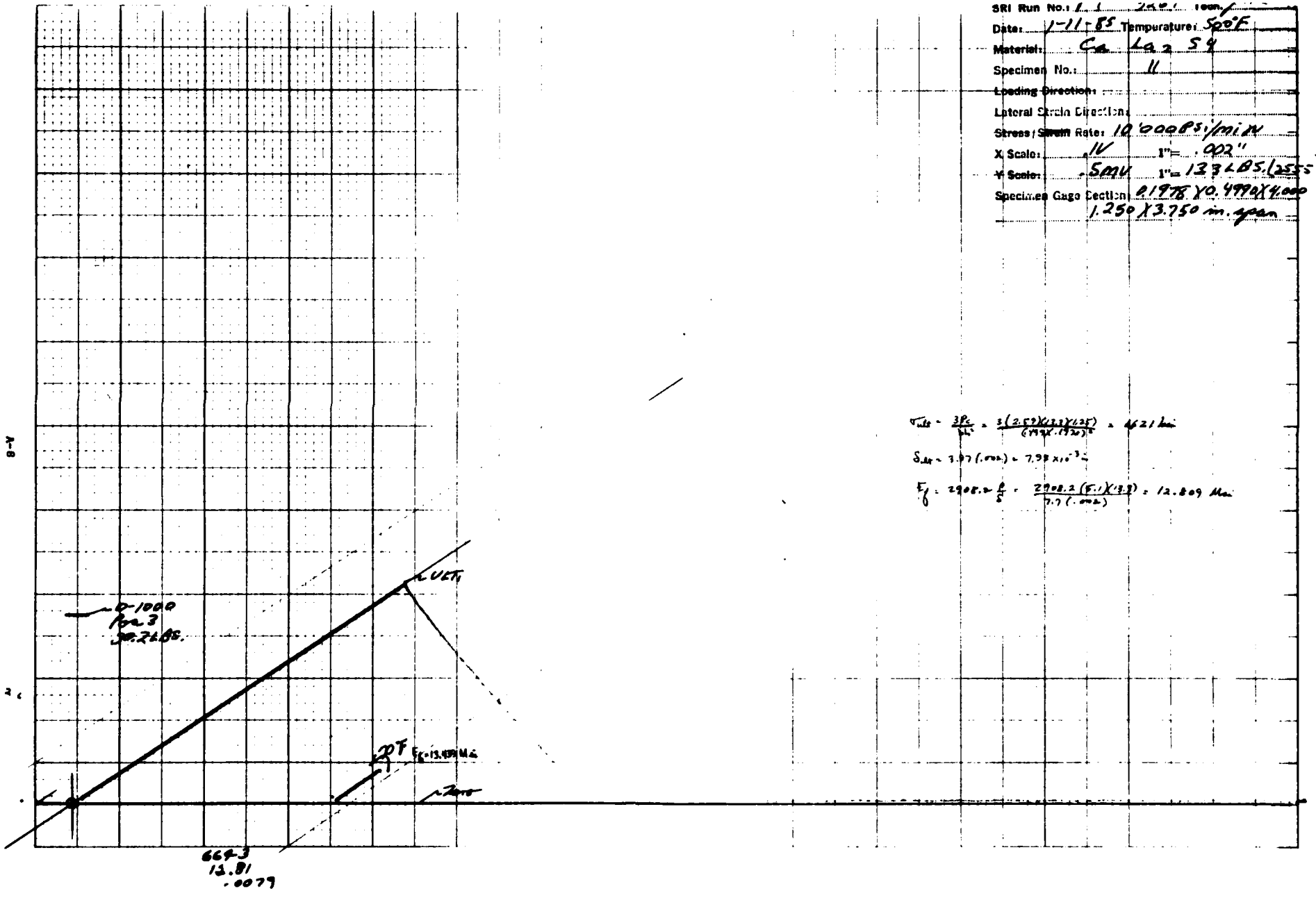

$\sigma_{ult} = \frac{3Pc}{bh^2} = \frac{3(2.59)(13.3)(1.25)}{(.199)(.1920)^2} = 4621$ ksi

$\delta_{ult} = 3.97(.002) = 7.93 \times 10^{-3}$ in

$E_f = 2908.2 \frac{P}{\delta} = \frac{2908.2(5.1)(13.9)}{7.7(.002)} = 12.809$ Msi

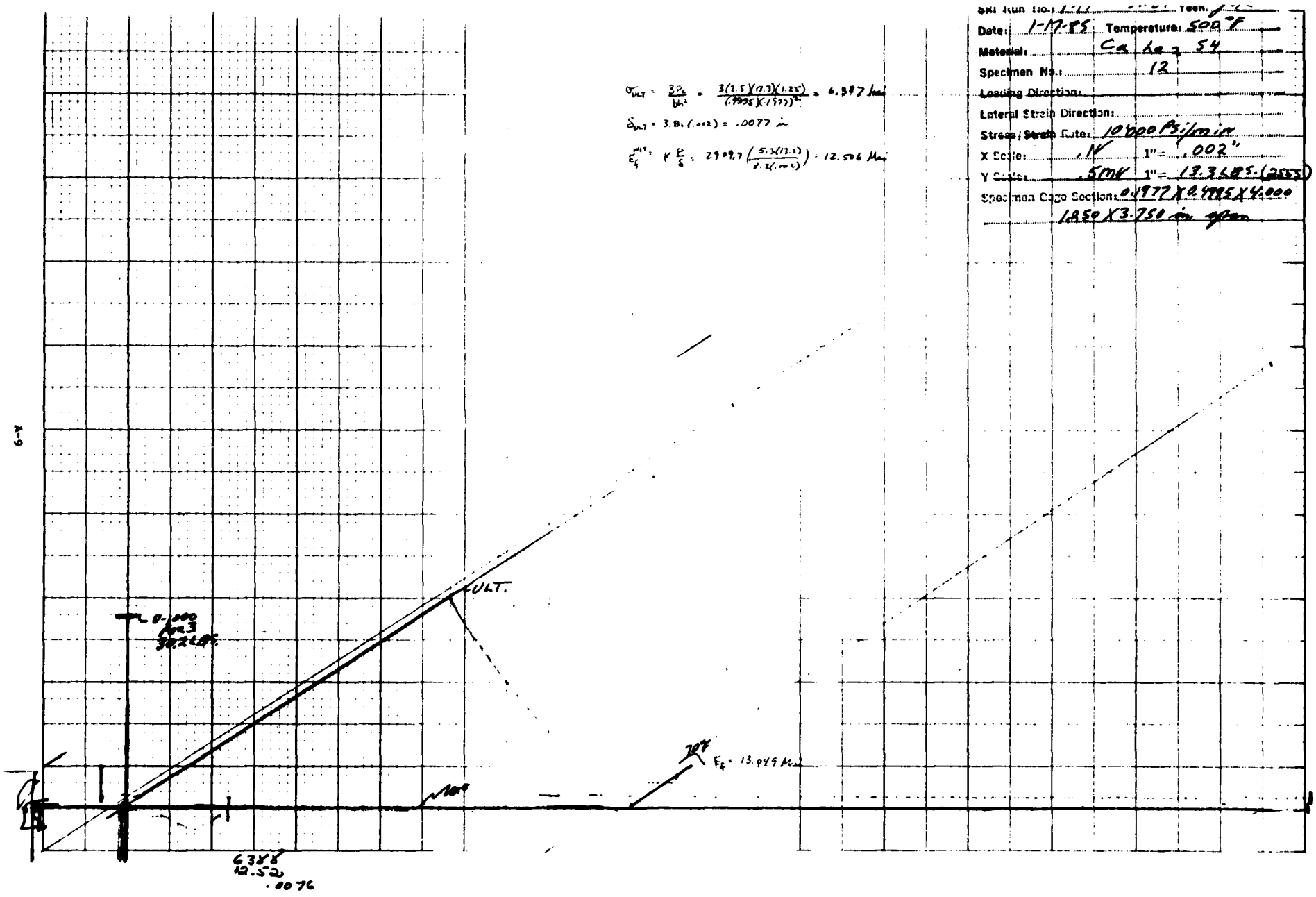

SKI Run No.:
Tech.:
Date: 1-17-85
Temperature: 500°F
Material: Ca La2 S4
Specimen No.: 12
Loading Direction:
Lateral Strain Direction:
Stress/Strain Rate: 10000 Psi/min
X Scale: .1V 1" = .002"
Y Scale: .5MV 1" = 13.3 LBS. (2555)
Specimen Gage Section: 0.1977 X 0.4995 X 4.000
1.250 X 3.750 in. span
$\sigma_{ULT} = \frac{3P_c}{bh^2} = \frac{3(2.5)(13.3)(1.25)}{(.4995)(.1977)^2} = 6.387$ ksi
$\delta_{ULT} = 3.8 \times (.002) = .0077$ in
$E_f^{INIT} = K\frac{P}{\delta} = 2909.7\left(\frac{5.3(13.3)}{8.2(.002)}\right) = 12.506$ Msi
ULT.
0-1000
Pos 3
30.2 LBS.
70°F
$E_f = 13.049$ Msi
6388
12.52
.0076

SRI Run No.: [illegible] Tech. [illegible]

Date: 1-10-85 Temperature: 500°F

Material: Ca La2 54

Specimen No.: 15

Loading Direction:

Lateral Strain Direction:

Stress / Strain Rate: 10'000 Psi/min

X Scale: .1V 1" = .002"

Y Scale: .5mV 1" = 13.3 LBS. (2662)

Specimen Gage Section: 0.1960 X 0.4990 X 4.000

1.250 X 3.750 in. span

$\sigma_{ult} = \frac{3Pc}{bh^2} = \frac{3(6.56)(13.3)(1.25)}{(.499)(.196)^2} = 4.054$ ksi

$\delta_{ult} = 2.34(.002) = 4.68 \times 10^{-3}$ in

$E_f = 2989.0 \frac{P}{\delta} = \frac{2989(4.1)(13.3)}{6.1(.002)} = 13.360$ Msi

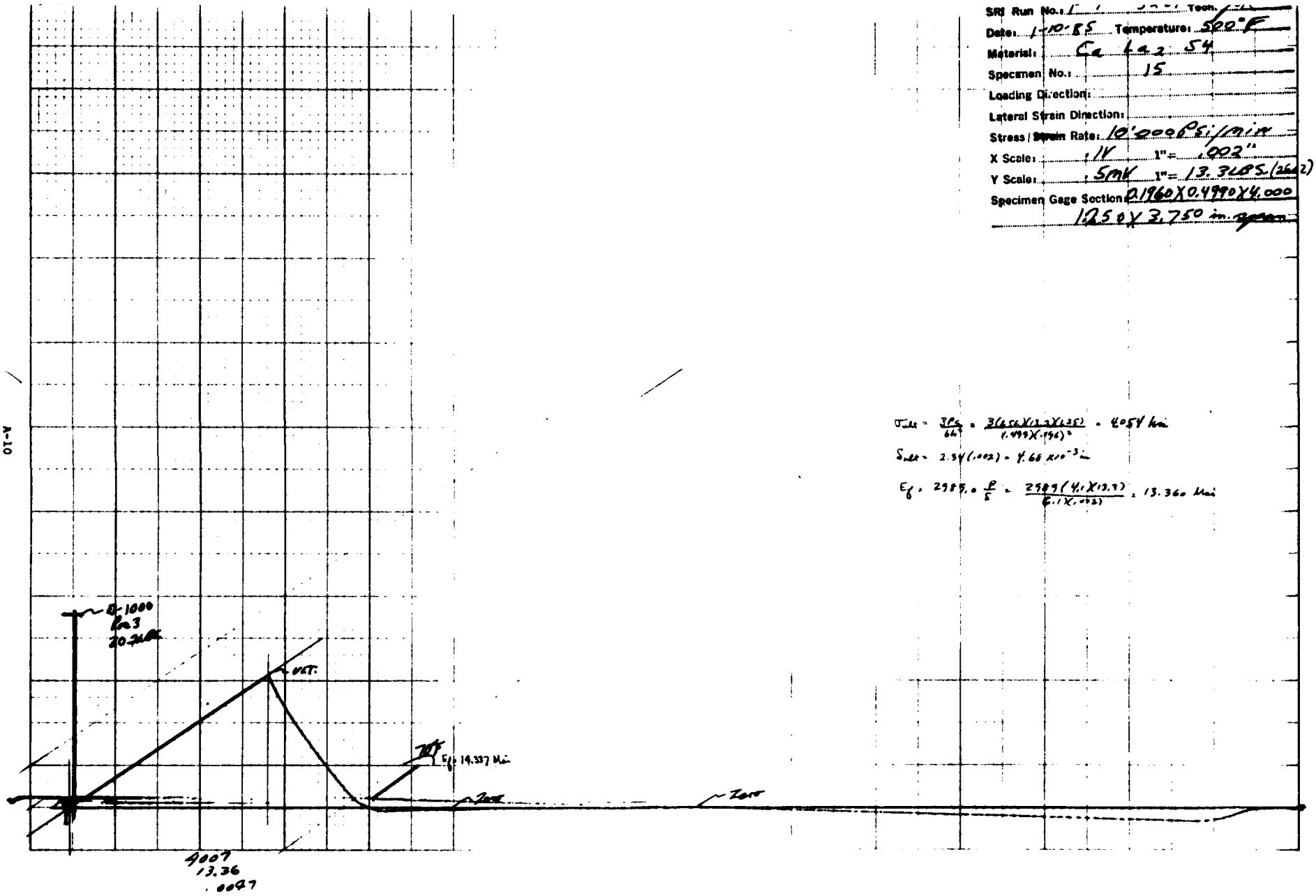

Date: 1-9-85 Temperature: 1600°F

Material: Ca La2 S4

Specimen No.: 3

Loading Direction:

Lateral Strain Direction:

Stress/~~Strain~~ rate: 10'000 psi/min

X Scale: .1V 1" = .002"

Y Scale: .5MV 1" = 13.3 LBS (2543)

Specimen Gage Section: 0.1982 x 0.4992 x 4.000

1.25 x 3.75 in. span

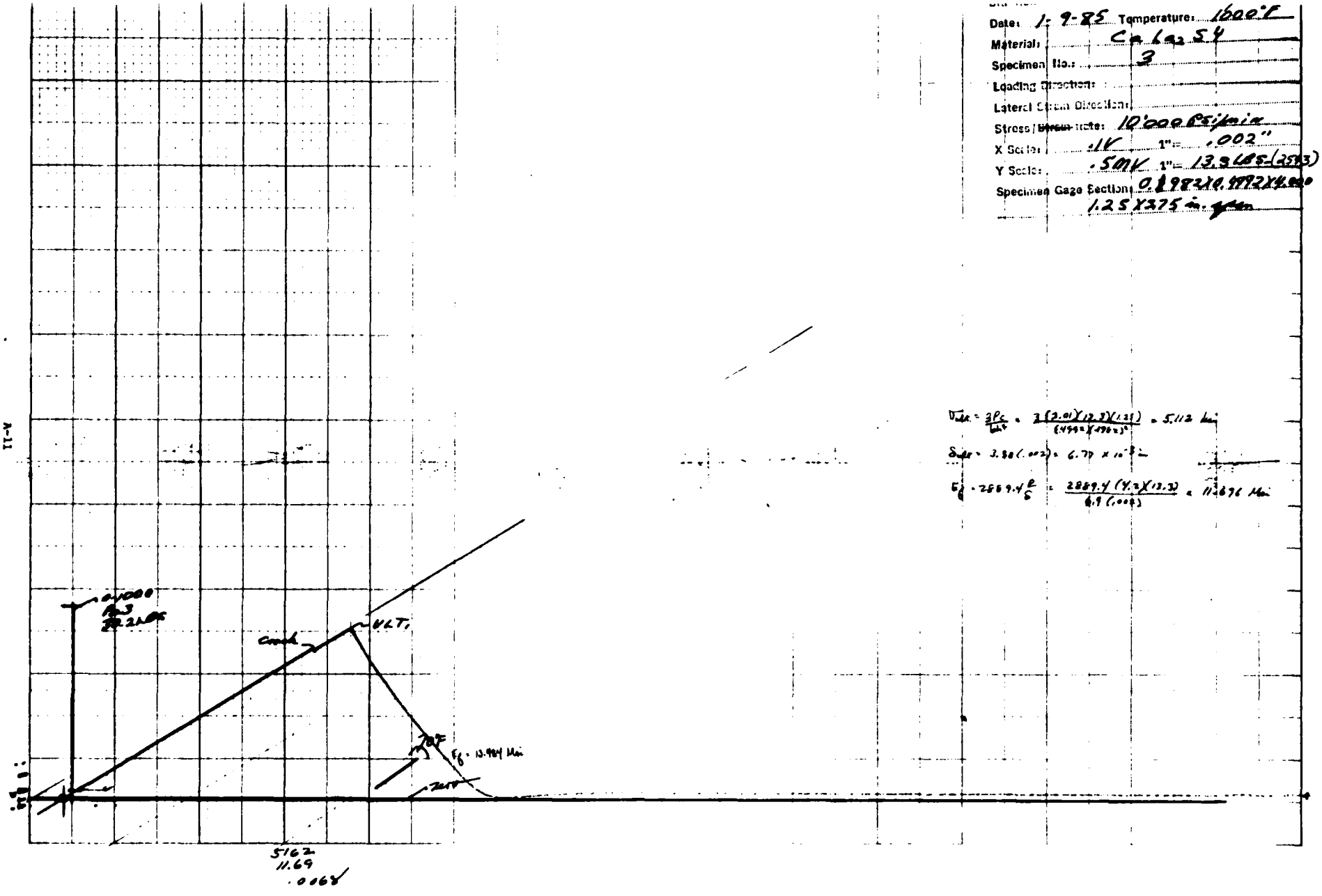

$\sigma_{ult} = \frac{3Pc}{bh^2} = \frac{3(2.01)(13.3)(1.25)}{(.4992)(.1982)^2} = 5.112$ ksi

$\delta_{ult} = 3.38(.002) = 6.77 \times 10^{-3}$ in

$E_f = 2889.4 \frac{P}{\delta} = \frac{2889.4(4.2)(13.3)}{6.9(.002)} = 11.696$ Min

SRI Run No.: F-5 5267 Tech. [illegible]

Date: 1-9-85 Temperature: 1000°F

Material: Ca La2 S4

Specimen No.: 7

Loading Direction:

Lateral Strain Direction:

Stress/Strain Rate: 10,000 psi/min

X Scale: .1V 1" = .002"

Y Scale: .5mV 1" = 13.3 LBS. (2550)

Specimen Gage Section: 0.1970 X 0.6000 X 4.000

1.25 X 3.75 in. span

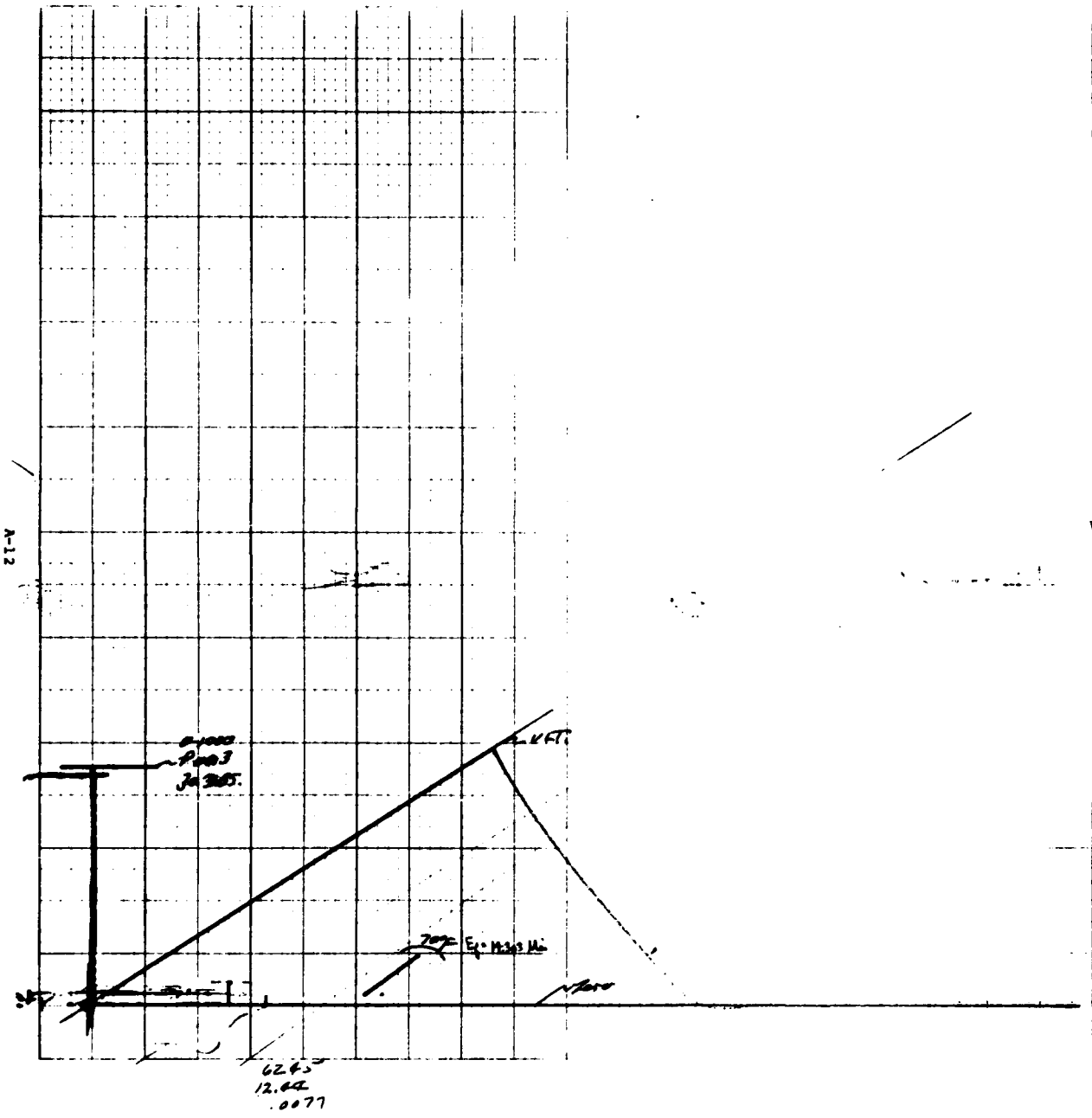

$\sigma_{ult} = \frac{3Pl}{bh^2} = \frac{3(2.43)(1.25)(13.3)}{(.500)(.197)^2} = 6.238$ ksi

$\delta_{ult} = 3.85(.002) = 7.70 \times 10^{-3}$ in

$\varepsilon_f = 2937.8 \frac{P}{b} = \frac{2937.8(4.6)(13.3)}{(2.2)(.002)} = 12.482$ Min

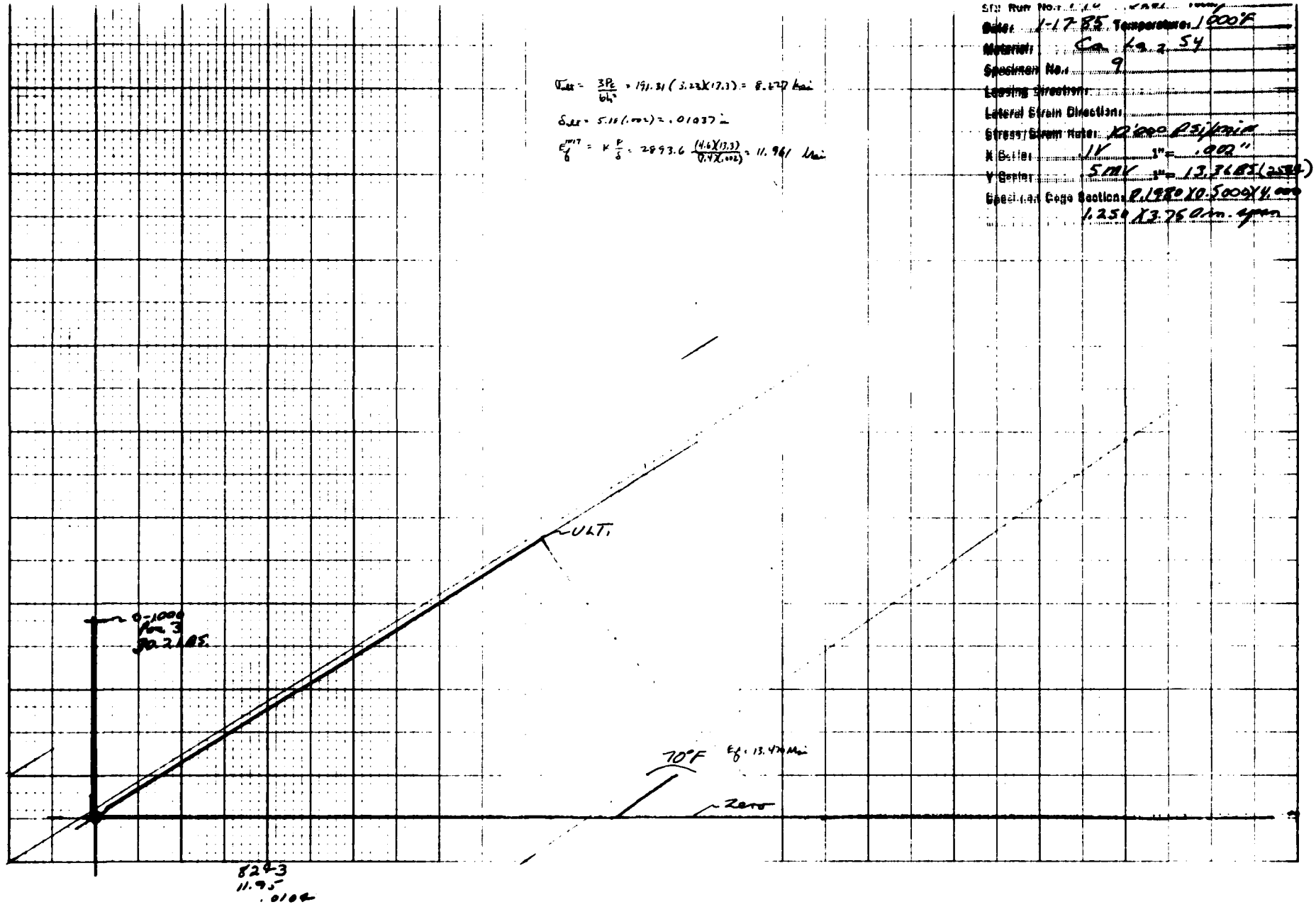

Date: 1-17-85 Temperature: 1000°F
Material: Ca La 2 S4
Specimen No.: 9
Lateral Strain Direction:
Stress/Strain Rate: 10'000 psi/min
X Scale: .1V 1" = .002"
Y Scale: .5mV 1" = 13.36 BS (2534)
Specimen Gage Section: 0.1980 X 0.5000 X 4.000
1.250 X 3.750 in. span
$\sigma_{ult} = \frac{3P_c}{bh^2} = 191.31(3.23)(17.3) = 8.227$ ksi
$\delta_{ult} = 5.18(.002) = .01037$ in
$E_f^{init} = K\frac{P}{\delta} = 2893.6\frac{(4.6)(13.3)}{(7.4)(.002)} = 11.961$ Msi
ULT.
0-1000
for 3
30.2 LBS.
70°F
Ef: 13.470 Msi
Zero
8243
11.95
.0104

Test Run No.: 1-15 2267 Tech. [illegible]

Date: 1-15-85 Temperature: 1000°F

Material: Ca La 2 S4

Specimen No.: 13

Loading Direction:

Lateral Strain Direction:

Stress/Strain Rate: 10'000 PSI/min

X Scale: .1V 1" = .002"

Y Scale: .5MV 1" = 13.3 LBS (25-59)

Specimen Gage Section: 0.1965 X 0.4990 X 4.000

1.25 X 3.75 in. span

Graphite load blocks

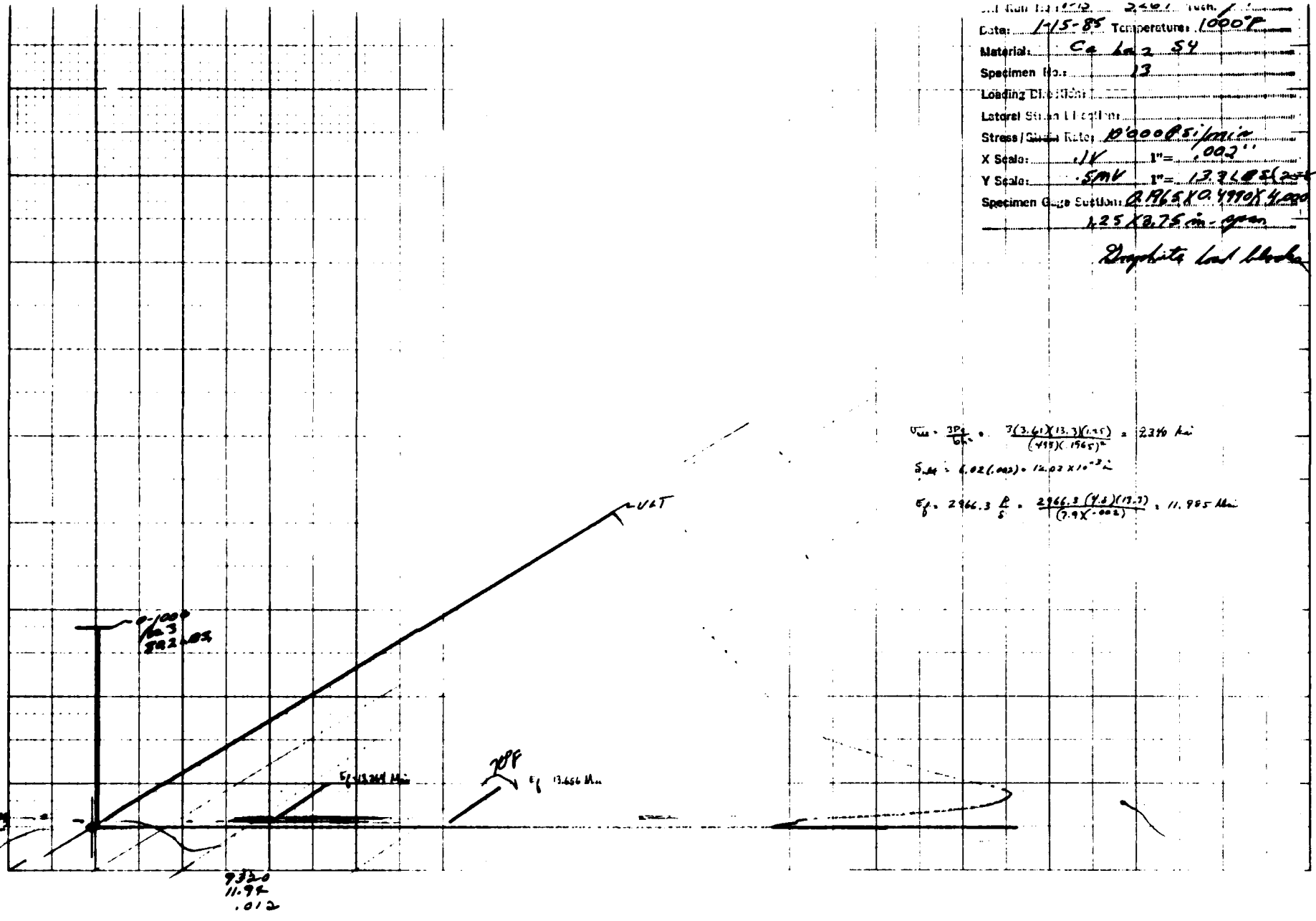

$\sigma_{ult} = \frac{3Pl}{bh^2} = \frac{3(3.61)(13.3)(1.25)}{(.495)(.1965)^2} = 2340$ ksi

$\delta_{ult} = 6.02(.002) = 12.02 \times 10^{-3}$ in

$E_f = 2966.3 \frac{P}{\delta} = \frac{2966.3(4.8)(13.3)}{(7.9)(.002)} = 11.985$ Msi

SRI Run No.: [illegible] Tech. [illegible]

Date: 1-10-85 Temperature: 1500°F

Material: Ca La2 S4

Specimen No.: 4

Loading Direction:

Lateral Strain Direction:

Stress/Strain Rate: 10,000 psi/min

X Scale: .1V 1" = .002"

Y Scale: .5mV 1" = 13.3 LBS (2527)

Specimen Gage Section: 0.1976 X 0.4995 X 4.000

1.25 in. X 3.750 in. span

$\sigma_{ult} = \frac{3Pa}{wh^2} = \frac{3(4.85)(12.3)(1.25)}{(.4995)(.1976)^2} = 12.403$ ksi

$\delta_{ult} = 4.85(.002) = 23.67 \times 10^{-3}$ in

$E_f^{III} = 2914.1 \frac{P}{\delta} = 2914.1 \frac{(4.2)(13.3)}{(7.9)(.002)} = 10.303$ Msi

$E_f^{II} = 2914.1 \frac{P}{\delta} = 2914.1 \frac{(4.5)(12.3)}{(2.7)(.002)} = 7.148$ Msi

$\gamma_{Poisson\ fit} = 2.42(.002) = 6.83 \times 10^{-3}$ in

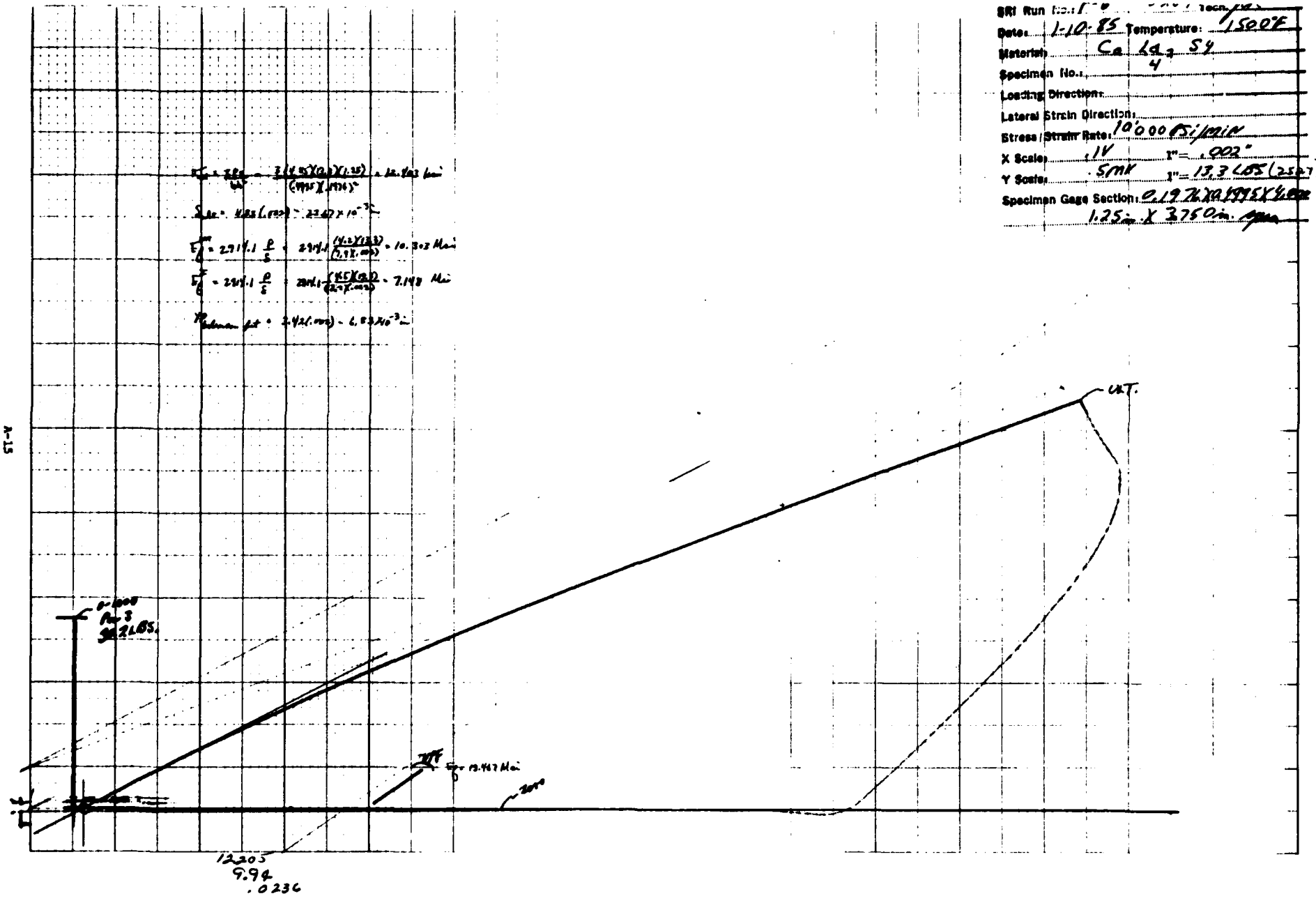

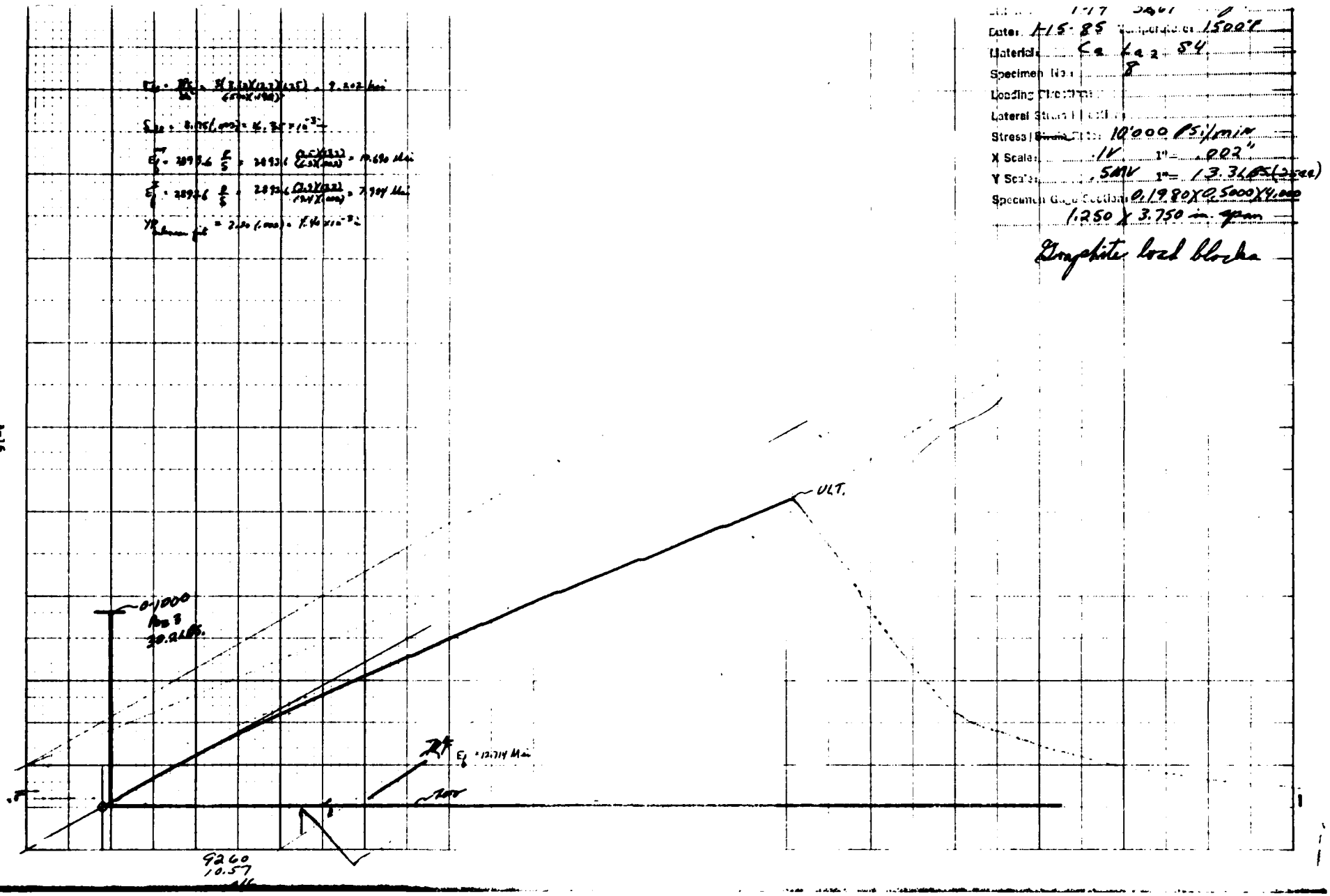
Date: 1-15-85
Temperature: 1500°F
Material: Ca La2 S4
Specimen No.: 8
Loading Direction:
Lateral Strain Location:
Stress/Strain Rate: 10'000 PSI/min
X Scale: .1V 1" = .002"
Y Scale: .5MV 1" = 13.3 LBS (2 sec)
Specimen Gage Section: 0.1980 X 0.5000 X 4.000
1.250 X 3.750 in. span
Graphite load blocks
ULT.
0-1000
30.2 LBS.
9260
10.57

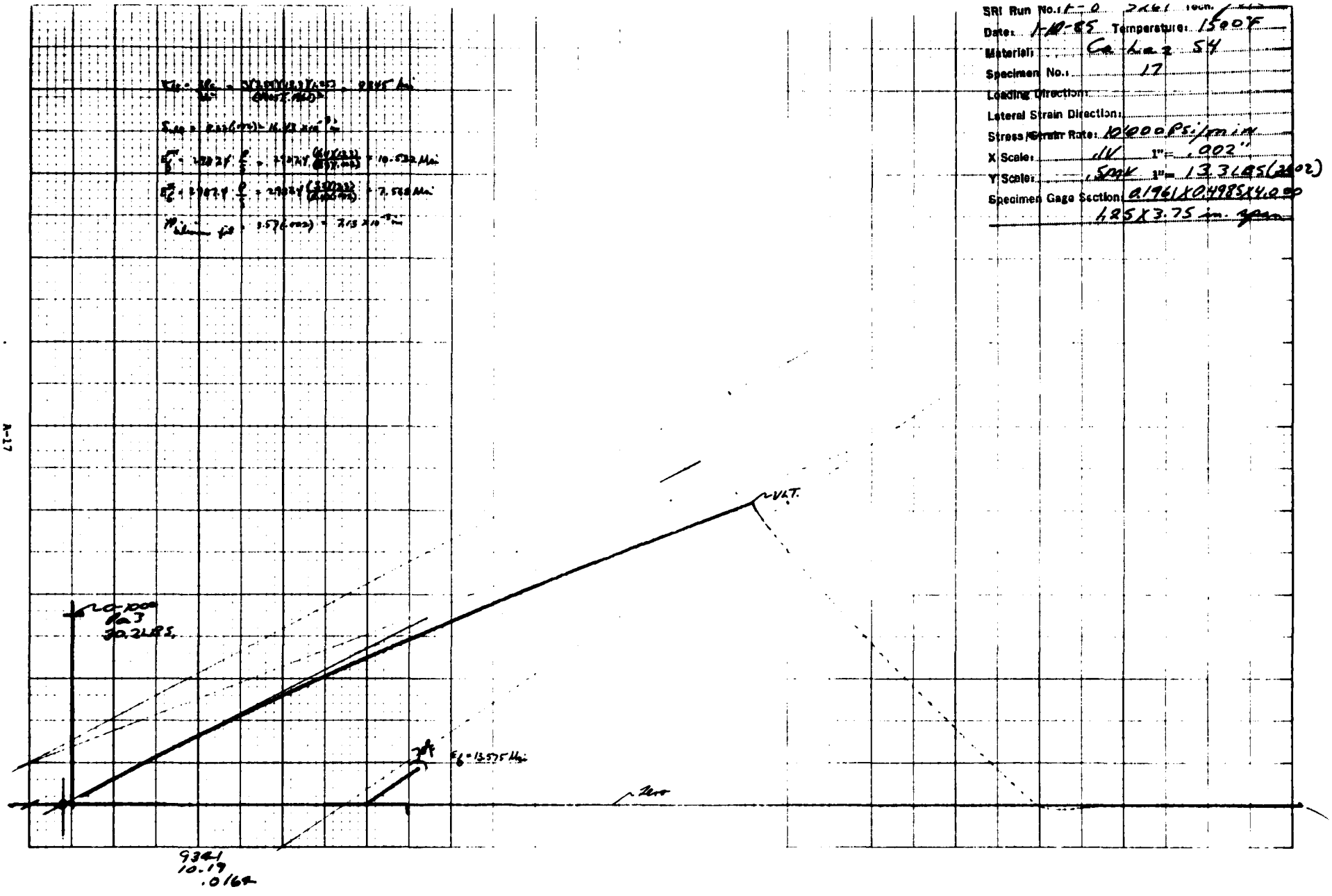
SRI Run No.: F-0 3261 Tech.
Date: 1-10-85 Temperature: 1500°F
Material: Ca Lac 54
Specimen No.: 17
Loading Direction:
Lateral Strain Direction:
Stress/Strain Rate: 10,000 psi/min
X Scale: .1V 1" = .002"
Y Scale: .5mV 1" = 13.3 LBS (.002)
Specimen Gage Section: 0.1961 X 0.4985 X 4.000
1.25 X 3.75 in. span
VLT.
Zero
9341
10.19
.0164

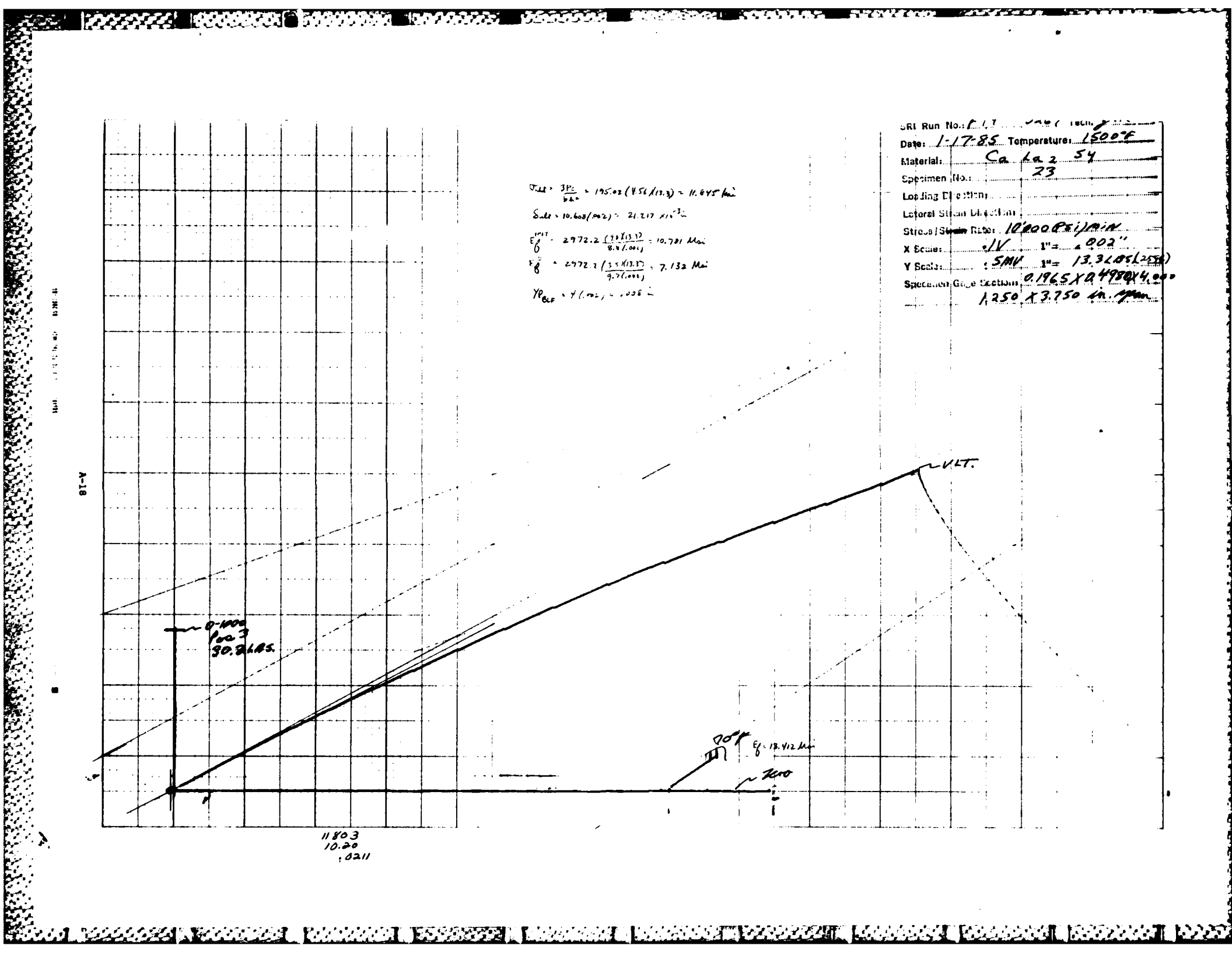
SRI Run No.:
Date: 1-17-85 Temperature: 1500°F
Material: Ca La 2 54
Specimen No.: 23
Loading Direction:
Lateral Strain Direction:
Stress/Strain Rate: 10,000 PSI/MIN
X Scale: .1V 1" = .002"
Y Scale: .5MV 1" = 13.3 LBS (25%)
Specimen Gage Section: 0.1965 X 0.4980 X 4.000
1.250 X 3.750 in. span
ULT.
ZERO
11803
10.20
.0211

Date: 1-18-85 Temperature: 1800°F

Material: Ca La2 S4

Specimen No.: 20

Loading Direction:

Lateral Strain Direction:

Stress/~~Strain~~ Rate: 10,000 PSI/min

X Scale: .1V 1" = .002"

Y Scale: .5MV 1" = 13.31 LBS. (2600)

Specimen Gage Section: 0.1960 X 0.4993 X 4.000

1.250 X 3.750 in. span

Graphite load block

$E_f = K\frac{P}{\delta}$; $K = \frac{[3c^2 - 4c^2]}{4bL^3} = 2987.23$

$E_f^{ult} = 2987.23\left(\frac{3.4(13.3)}{8.5(.002)}\right) = 7.946$ Msi

$YP_{BLF} = 4.07(.002) = 8.14 \times 10^{-3}$ in

$E_f^{II} = 2987.23\left[\frac{1.8(13.3)}{7.8(.002)}\right] = 4.584$ Msi

$\sigma_{ult} = \frac{3Pc}{bL} = \frac{3(4(13.3))(1.250)}{(.4993)(.196)^2} = 10.401$ ksi

$\delta_{ult} = 15.35(.002) = 30.70 \times 10^{-3}$ in

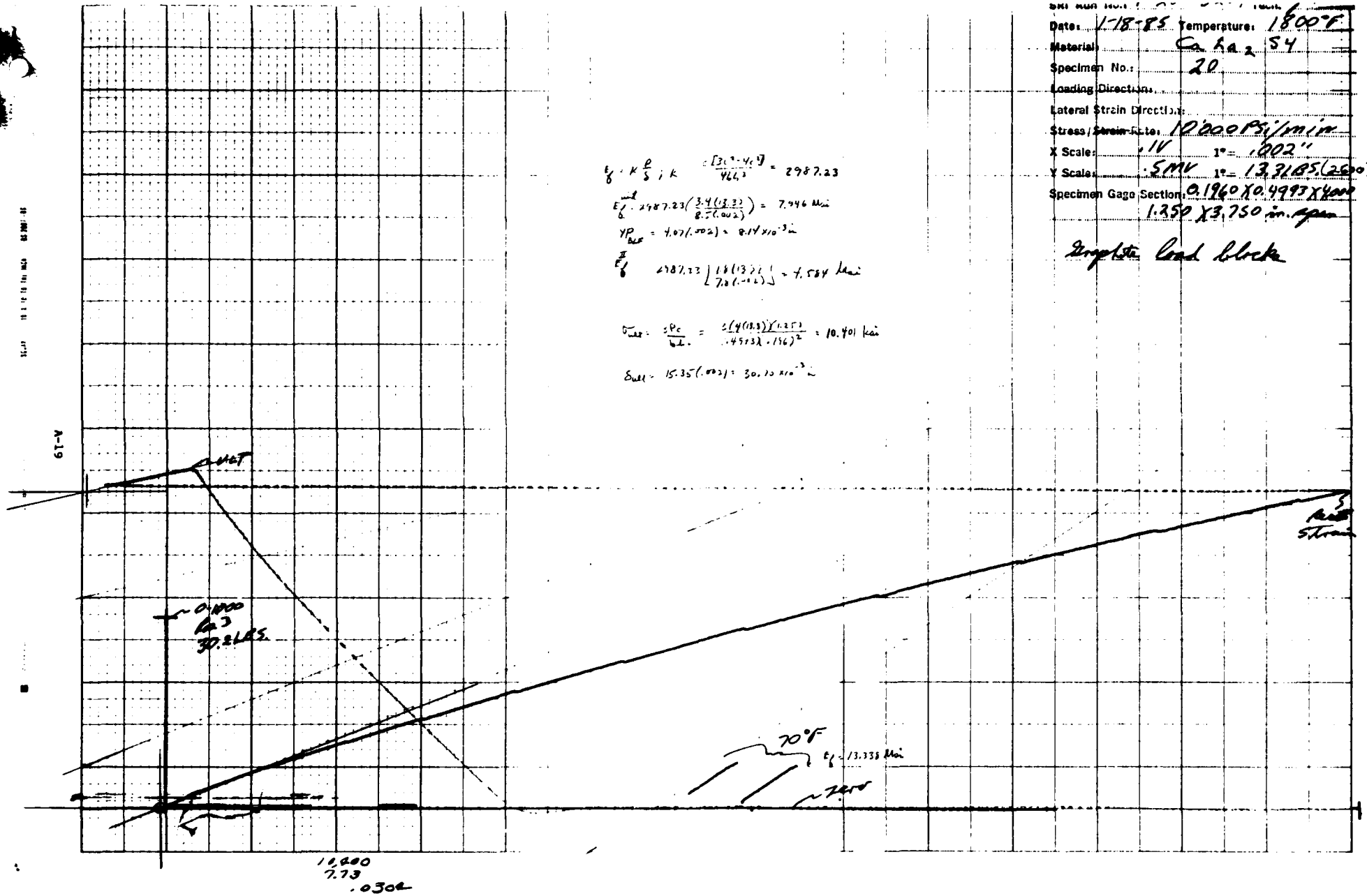

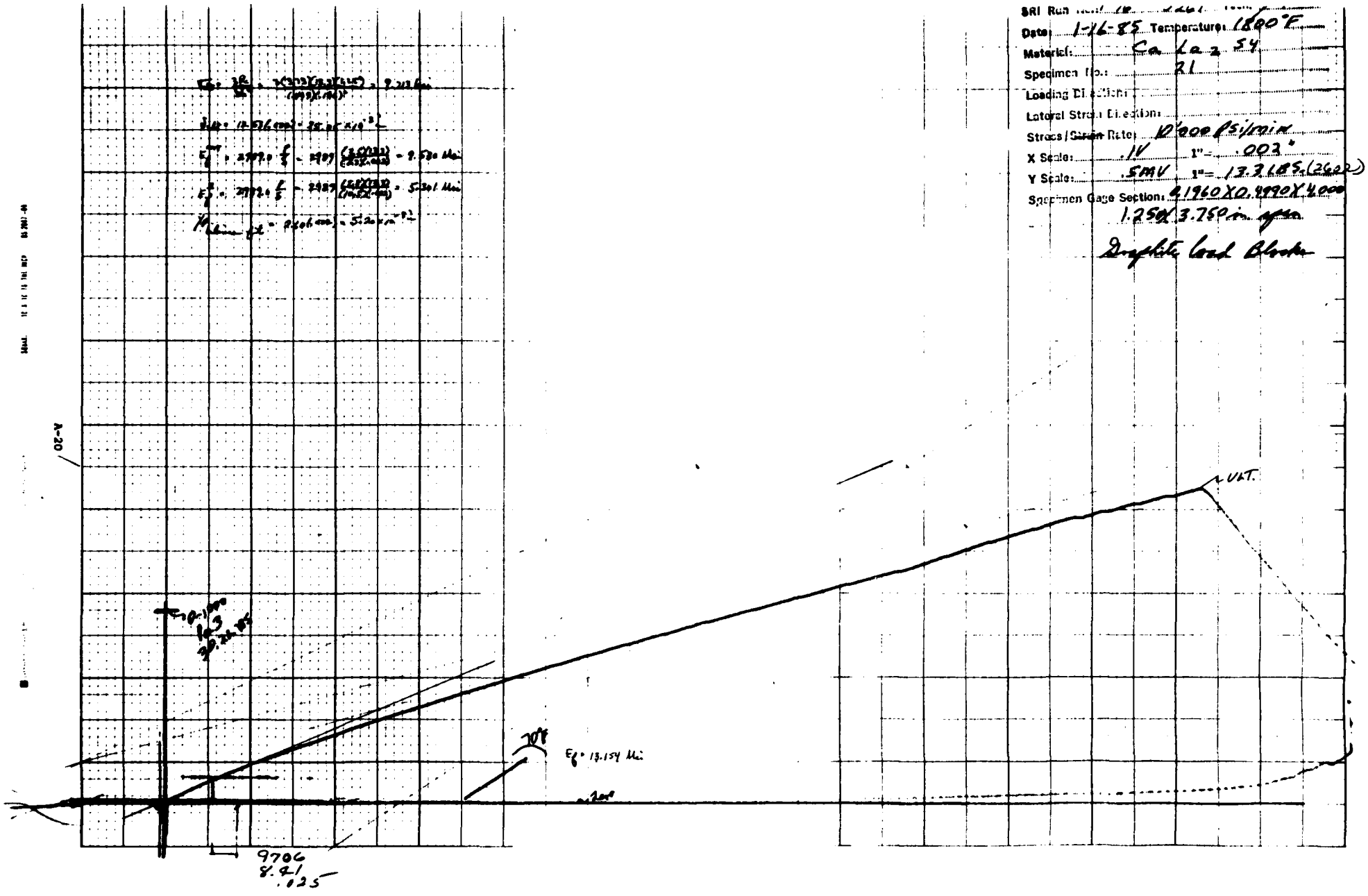
SRI Run
Date: 1-16-85 Temperature: 1800°F
Material: Ca La2 S4
Specimen No.: 21
Loading Direction:
Lateral Strain Direction:
Stress/Strain Rate: 10'000 psi/min
X Scale: .1V 1" = .002"
Y Scale: .5MV 1" = 13.3 LBS. (2602)
Specimen Gage Section: 0.1960 X 0.4990 X 4.000
1.250 X 3.750 in. span
Graphite Load Blocks
ULT.
70°F
Ef = 13.154 Mi
9706
8.41
.025

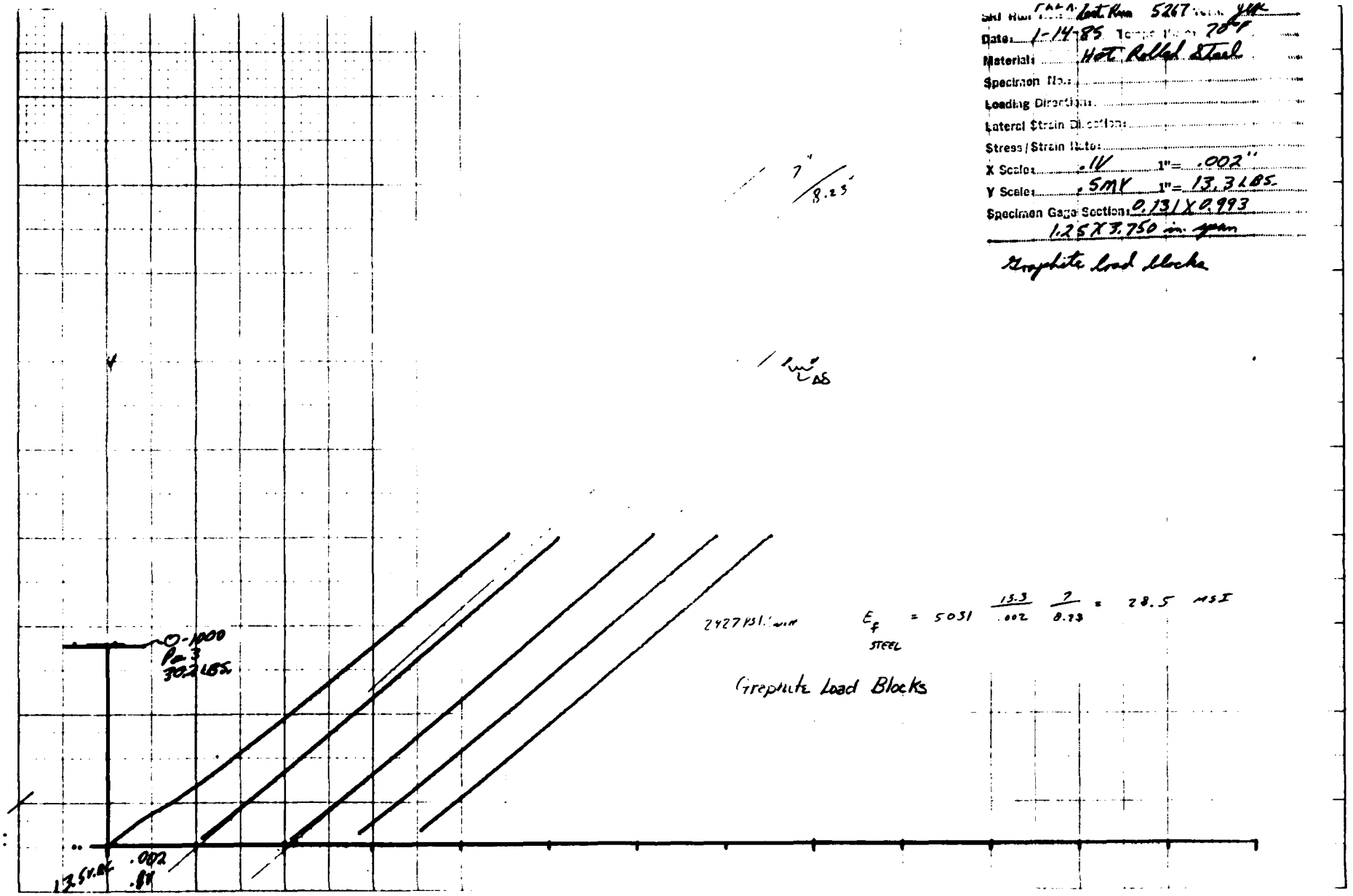

Date: 1-14-85
Material: Hot Rolled Steel
Specimen No.:
Loading Direction:
Lateral Strain Direction:
Stress/Strain Rate:
X Scale: .1V 1" = .002"
Y Scale: .5MV 1" = 13.3 LBS.
Specimen Gage Section: 0.131 X 0.993
1.25 X 3.750 in. span
Graphite load blocks
7"/8.23"
0-1000
Pa 3
30.2 LBS.
13.5 V.DC
.002
.8V
2427 PSI/min
$E_{f_{STEEL}} = 5031 \frac{13.3}{.002} \frac{7}{8.23} = 28.5$ MSI
Graphite Load Blocks

Date: 1-8-85 Temperature: 70°F

Material: Hot Rolled Steel

Specimen No.:

Loading Direction:

Lateral Strain Direction:

Stress/Strain Rate:

X Scale: .05V 1" = .001"

Y Scale: .5MV 1" = 13.3 LBS.

Specimen Gage Section: 0.13 X 0.993

1.25 X 3.75 in. span

5/11.55

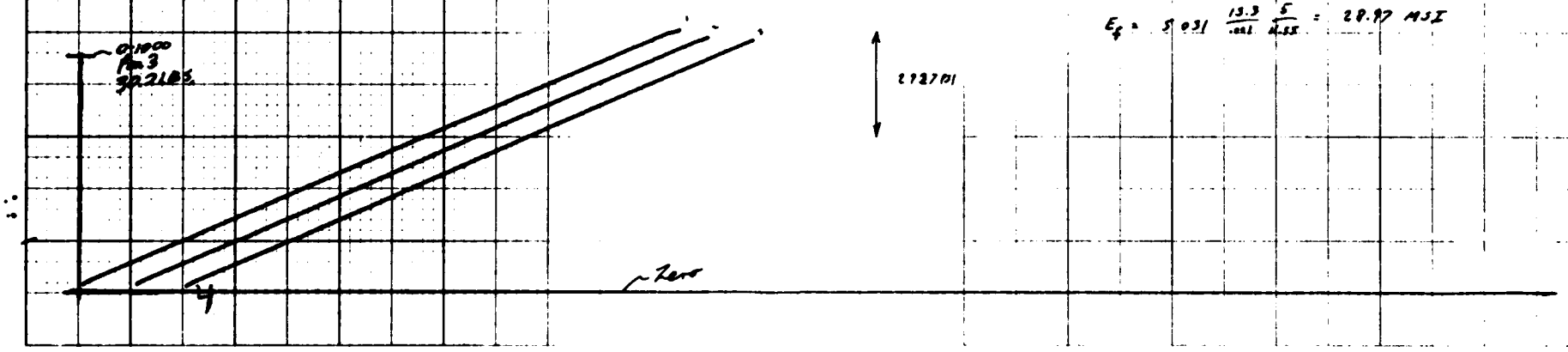

$E_f = 5.031 \frac{13.3}{.001} \frac{5}{11.55} = 28.97$ MSI

APPENDIX B

SENSITIVITY STUDIES

Sensitivity Studies

The sensitivity studies in Reference 1 were conducted on Pyroceram® using nominal properties available prior to the data set developed under that effort. The analysis was conducted on a radome structure at aerodynamic heating condition somewhat exceeding those anticipated for the IR windows for which the materials under this effort were evaluated. The analysis was conducted using state of the art aerodynamic heating codes, the Asthma code for indepth heating analysis and SAAS-III body of revelation finite element structural analysis. The material properties were modeled as elastic with equal tensile and compressive moduli which varied as a function of temperature.

Prior to initiating the testing effort, the peak stressed volumes and areas were calculated. These were comparable to the tensile specimens used in that effort. Note that the volume and surface areas are about the same as would be involved in the ID surface of an IR Dome despite the much larger size of the full radome as shown in Figure 1.

The sensitivity studies were conducted by varying the properties listed in Table 1 one at a time. As can be seen the most sensitive parameters in terms of stress generation were the stiffnesses and thermal expansion.

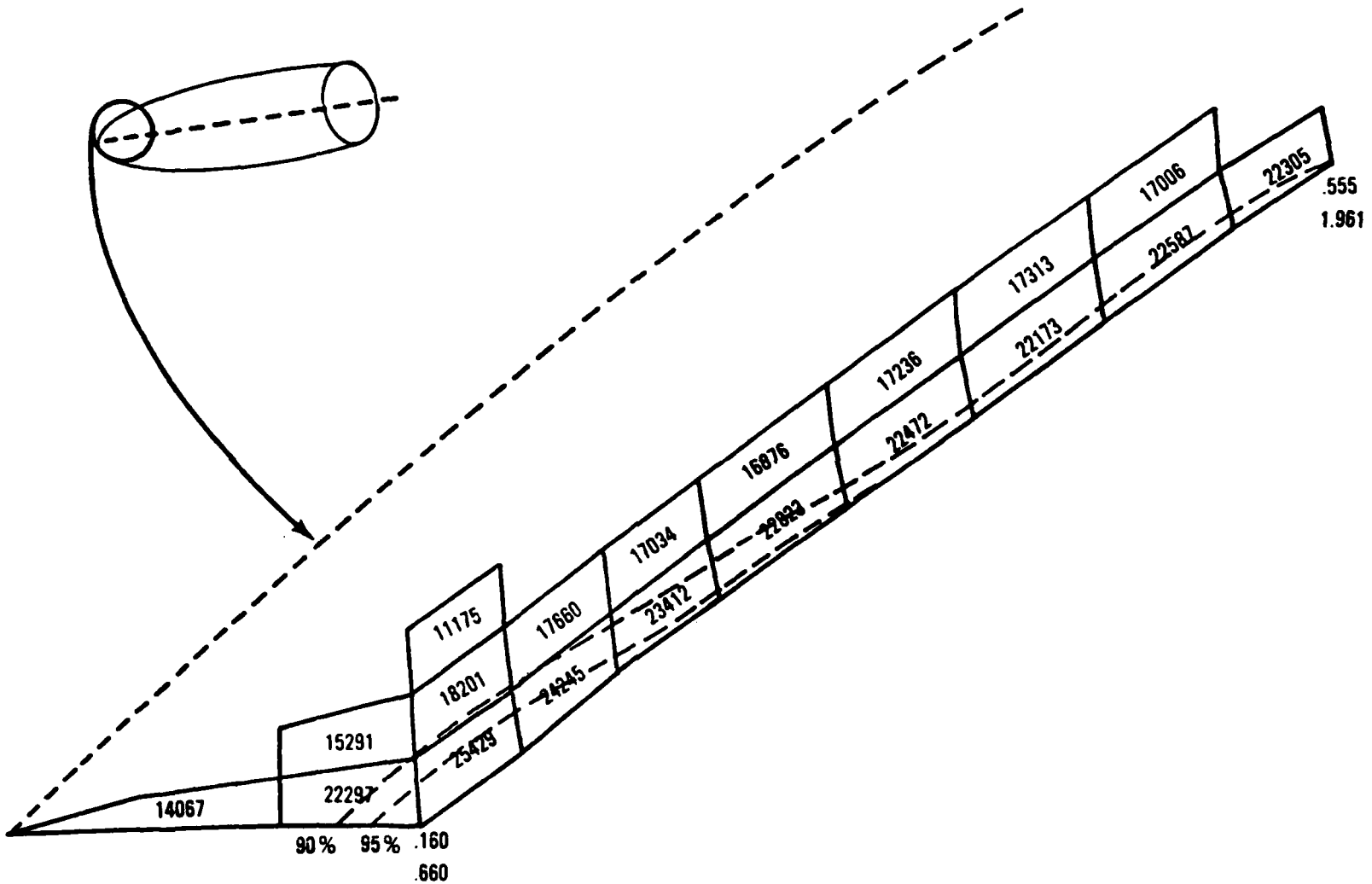

Figure 1. Peak stressed volume and surface area for Radome in Reference 1

Table 1. Sensitivity Study Summary

ERROR INTRODUCED	PARAMETER	ERROR IN BACK FACE TEMP. RISE	ERROR IN MAX THETA STRESS
5%	VELOCITY	10%	9%
5%	THERMAL CONDUCTIVITY	1.2%	1.2%
5%	THICKNESS	1.5%	1.5%
100%	EMISIVITY	0.1%	0.1%
1/8"	STRAIN GAUGE LOCATION		6%
1/8"	THERMO COUPLE LOCATION	8.5%	
			6.2%
			3%
−15% BASELINE	MODULUS		−15%
+11% BASELINE	MODULUS		+11%
+11% CONSTANT F(T)	MODULUS		+4%
LINEAR/2 nd SLOPE	EXPANSION		−3%
−30% LINEAR/2 nd SLOPE	EXPANSION		−34%
−40% LINEAR/2 nd SLOPE	EXPANSION		−47%
−50% LINEAR/2 nd SLOPE	EXPANSION		−52%

END

FILMED

12-85

DTIC